JONAS
Joint Framework for Ocean Noise in the Atlantic Seas

Deliverable 8.3 - Seismic survey noise prediction tool.

Project Name	JONAS
Project ID	INTERREG ATLANTIC - Contract EAPA 51/2018
Document name	Deliverable 8.3 - Seismic survey noise prediction tool.
Document version	1.0
Author	Ricardo Duarte, Giulia Spadoni and Sérgio M. Jesus
Supervisor	JONAS
Date	April 2022
Status	PU (for Public)

Nomenclature

Ax.y	Action y of work package x
CIR	Channel Impulse Response
DEM	Digital Elevation Model
Dx.y	Deliverable y of work package x
EC	European Commission
ENM	Environmental Niche Models
EOV	Essential Ocean Variable
ESAS	European Seabirds at Sea
EU	European Union
GOOS	Global Ocean Observation System
GPS	Global Positioning System
HF	High-frequency
HS	Habitat Suitability
JONAS	Joint Framework for Ocean Noise in the Atlantic Seas
MF	Mid-frequency
MI	MarIlimitado
MSA	Minimum Sampled Area
MSFD	Marine Strategy Framework Directive
OSPAR	Oslo and Paris Conventions
PC	Project Coordinator
PI	Principal Investigator
PTS	Permanent Threshold Shift
PMO	Project Management Office
SDM	Species Distribution Modeling
SEAEO	Sea and Estuary Odyssey
SEL	Sound Exposure Level
SPEA	Sociedade Portuguesa para o Estudo das Aves
SPL	Sound Pressure Level
SSP	Sound Speed Profile
SST	Sea Surface Temperature
TL	Transmission Loss
TOL	1/3-Octave Band Level
TTS	Temporary Threshold Shift
WPx	Work Package x
WW	Whale Watching

Executive Summary

There is a consensus that anthropogenic ocean noise has increased worldwide over the past 50 years as a result of human maritime activities, in particular due to a significant increase of ship traffic, and as a result of the endless quest for energy, both of fossil and more recently also renewable origin, among others.

Efforts to assess and mitigate underwater noise resulting from anthropogenic sources should be an endeavour of EU member states towards a higher protection of biodiversity and marine life. Ocean sound has now been declared as an essential ocean variable (EOV) by the Global Ocean Observation System (GOOS), which goes in line with the efforts made by countries to protect their oceans and marine species.

JONAS project addresses the impact of underwater noise on sensitive species and the potential threat to biodiversity in the EU North Atlantic area, which has levels of ship traffic and marine activity among the highest in the world.

For ocean noise characterization, it is commonly accepted to separate continuous noise, such as that produced by shipping, which is ubiquitous, indistinct and often of relatively low level, and impulsive noise which is normally temporary, localized in space and of high or very high intensity. Among the activities generating impulsive noise there is seismic surveying for oil and gas exploration, and now also for offshore renewable energy installations. Seismic surveying for oil and gas generally aims at identifying large deposits deep into the bottom and its effects have been thoroughly reported in the literature. Instead, the environmental effects of light seismic surveying, that aims at superficial bottom sediment structure identification, has not been. Light seismic surveying has substantially different characteristics, covers different areas and may, therefore, have a quite different impact on marine life.

In the fulfillment of the requirements of task A8.3 of project JONAS, this report describes a tool for evaluating the impact of light seismic surveys in shallow water. This tool has three components: first, a model-based methodology for determining sound pressure level distribution due to a seismic survey in a given area; second, the evaluation of species' habitat suitability in the same area, using the Environmental Niche Method; and third, the combination of noise distribution and habitat suitability to provide a quantifiable and comparable risk assessment for that species in that particular habitat.

This tool is applied in a realistic simulated survey taking place in a selected area of the SW coast of Portugal, where environmental and biological data was available. Final validation of the tool against experimental data could not be performed, but a few conclusions can be drawn: as expected sound exposure levels (SEL) in the area of the seismic survey may reach exceptionally high values relative to normally accepted temporary / permanent threshold shifts of hearing perception of various species; acoustic energy is strongly attenuated in shallow water but may still impact communities in a roughly 40x40 km platform area around the seismic survey zone.

All in all, the proposed tool provides a first assessment of the shallow water seismic survey impact with quantifiable and comparable risk outputs, which may be used for area management decision support.

Abstract

Underwater noise is an important form of pollution in the ocean, that puts at risk a considerable number of marine species. One of the major contributors to underwater noise is seismic exploration, that is traditionally used to detect offshore gas and oil deposits but also, in a "light" survey version, to map the superficial layers of the sea bottom, in order to plan for the installation of renewable (wind and wave) energy structures. The increasing use of light seismic surveying in coastal areas has drawn the attention for evaluating its impact on selected species. This study proposes a tool for estimating noise level distribution due to a shallow water seismic survey that, coupled with habitat suitability for a sensitive species, allows for risk assessment mapping. The simulation results on a test case area on the continental platform of the SW coast of Portugal, near Setúbal, show that: significant sound pressure levels may be attained in large swaths of the considered area; that impact on habitat suitability consistently follows noise distribution and that the proposed methodology for risk assessment may provide an alternative for obtaining comparable risk indicators.

Contents

1 Introduction

Ocean soundscape refers to the interaction between sound and the oceanscape including its natural physical and biological components as well as the sound generated by human activity, which over the past decades suffered a considerable increase [1].

It is known that marine species rely on sound to forage, to interact in community, to orientate and to perceive their surrounding environment. However, the continuous growth of pervasive and high intensity impulsive anthropogenic noise sources in the ocean increases the risk to the most exposed marine species.

One may divide anthropogenic noise in two categories: continuous noise, that encompasses the noise produced by ships, generally of low or moderate intensity, and impulsive noise, that is localized in space, but has usually high or very high intensity for limited periods of time. Examples of impulsive noise sources are pile driving for offshore construction, military and civilian sonar, and seismic surveying for oil and gas, among others [2]. The pervasive nature of continuous noise do not allows for animals to escape but its effects are generally at long term. Conversely, impulsive noise may have more devastating effects at short term and for localized areas where noise generating activities take place.

Classical seismic surveying for oil and gas generally aims at detecting large reservoirs deep (sometimes thousands of meters) into the ocean bottom so, employing low frequencies (100 Hz band or lower) and pulses are highly energetic (levels of 260 dB re 1μPa are not uncommon). As depicted in Fig. 1, sound sources and long arrays of hydrophones are towed by ships over the area of interest. The output is processed to obtain a bottom profile along range, and sometimes also cross-range for the 3D imaging case. Most "new" oil and gas deposits are now in deep water areas so, seismic activities for that purpose are frequently offshore.

Like many other countries, Portugal is on a voracious race for energy, and a few years ago has set plans for oil and gas harvesting concessions. The Portuguese Government has granted oil and gas exploration rights to the oil and gas industry for several offshore slots along all the coast of continental Portugal mainland as shown in Fig. 2. Preliminary seismic surveying was initially scheduled for the second half of 2018 [4].

There is a seismic surveying market developing also for coastal areas, aiming at providing estimates of bottom properties for installation of bridges, breakwaters, windmill platforms, wave energy generators or cabling infrastructures. This is sometimes referred to as light seismic surveying since the required bottom penetration is on the order of only a few tens of meters with, however, higher resolution, and involving relatively low energy sources. Because frequency bands are on the order of several hundred Hz up to a few kHz, sources are smaller than in the oil and gas case. There is some knowledge gap regarding the impact of light seismic surveys since, in one hand, levels are lower than in the oil and gas, which would point towards less impact, but on the other hand shallow water puts surveys closer to many protected areas, coastal communities, fishing areas, etc, which may lead to an increased impact.

Another relevant aspect for the Portuguese west coast is that it has relatively good conditions for the development of renewable offshore energy both using wave and/or wind, as mentioned in the Portugal's National Strategy for the Sea 2013–2020 that considers them as a strategic opportunity for the country. Therefore, offshore wind farm installations have been strongly encouraged in the area [6, 7].

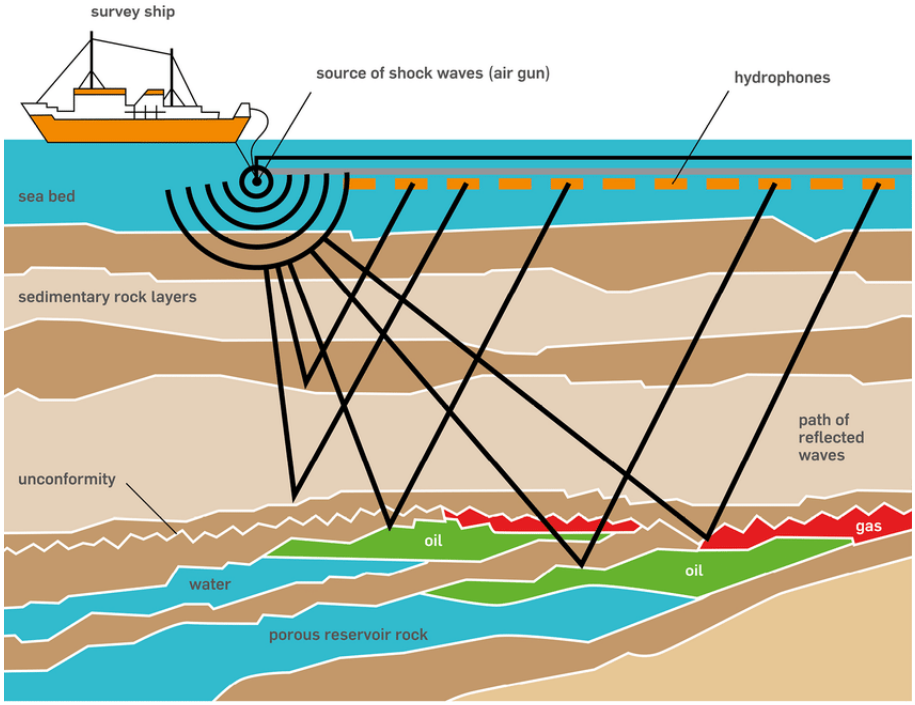

Figure 1: Example of a seismic survey experimental setup (adapted from [3]).

Finally, one should note that the Portuguese coast in general and the south-west coast of Portugal in particular, are areas of great marine biodiversity, high fishing activity due to the natural upwelling, and where every year a countless number of resident cetaceans are being sighted [8]. The land stretch along the SW coast has been declared as a protected natural park (Parque Natural do Sudoeste Alentejano e Costa Vicentina) since 1988.

In the framework of action "A8.3 - Seismic survey consenting decision support" of the JONAS program of work, the following aspects were pondered: the lack of knowledge on light seismic survey noise emissions, and the potential threat for seismic surveys to take place in or in the vicinity of a protected natural park. This has naturally lead to the choice of the area of the northern part of the SW-coast, near Setúbal, as test area for this study. A typical hypothetical light seismic survey was designed in the chosen realistic scenario characterized by environmental descriptors from archival data. A tool was developed for predicting sound exposure level (SEL) distribution based on acoustic propagation models' simulations. From a separate setting, Environmental Niche Models (ENM) were developed for the population of *Delphinus delphis* (*i.e. common dolphin*) to predict the habitat suitability (HS). Finally, SEL distribution and ENM outputs were combined using two different approaches to estimate the areas of potential risk for this species in two periods of the year.

The obtained results showed that significant sound pressure levels may be attained in large swaths of the considered area with impacts on habitat suitability for the chosen species. The deduced potential risk is consistent with the area distribution findings and gives hints for producing indicators and to support management activities.

This report is organized as follows: section 2 describes methodologies, data sets and

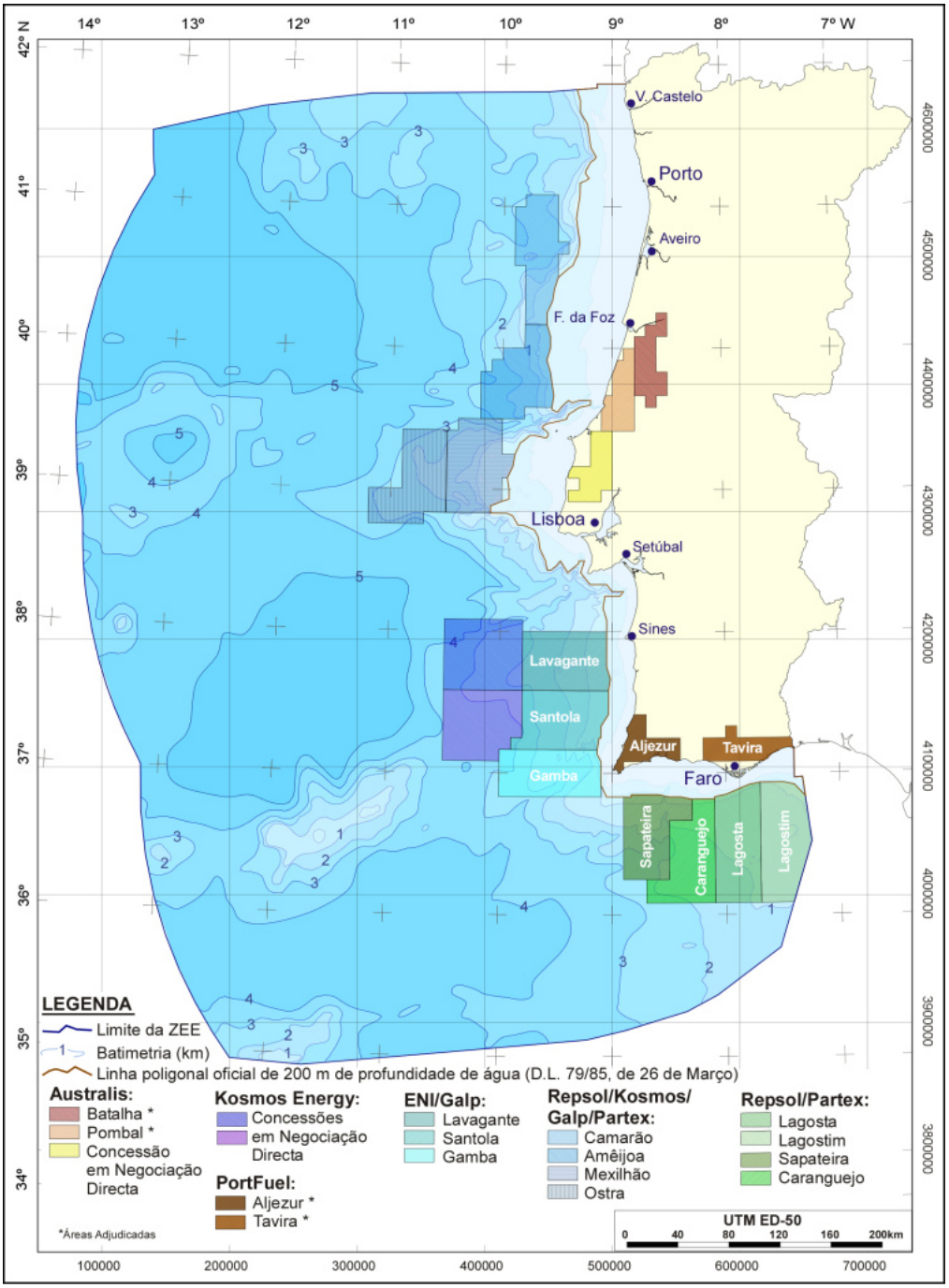

Figure 2: Considered offshore oil and gas exploration concessions (adapted from [5]).

setups for the developed and tested techniques; section 3 shows the obtained results for the various tests and simulation scenarios; section 4 gives a thoroughly account of the results and finally section 5 gives some conclusions and hints for future improvement.

2 Materials and methods

This section describes the physical environmental and biological properties of the Setúbal test case area as well as the methods and techniques used to: a) model a typical seismic survey scenario; b) model the habitat suitability for the particular case of the common dolphin; and c) estimate risk for common dolphin population based on the predictions both of seismic noise distribution and habitat suitability.

2.1 Physical and biological characteristics of the area

2.1.1 Bathymetry

Detailed bathymetry is a compulsory input to describe a specific environmental region and essential to obtain a realistic acoustic propagation model. The bathymetric data of the Portuguese coast was taken from the General Bathymetric Chart of Oceans (GEBCO) database [1], with a 15 arc-second interval generated by the assimilation of heterogeneous data, all referred to the mean sea level [9]. The study area of interest was limited to -9.3 and -8.5 longitude west and 38.2 and 38.6 latitude north as shown in Fig. 3 with a spatial resolution of 1 km x 1 km. The bathymetry of the target area presents an almost flat continental platform extending up to approximately 45 km from the coastline where the water depth reaches 250 m and then rapidly increases to the deeper ocean to the west. An interesting feature is the Setúbal canyon, a east-west oriented steep-sided valley at approximately 38.2º latitude north, that entails the platform with depths reaching 1000 m.

2.1.2 Bottom and sub-bottom properties

Site-specific bottom and sub-bottom acoustic properties are generally extremely difficult to obtain. Fortunately the study area was previously used for acoustic experiments during which acoustic bottom parameters were identified. A two layer bottom model composed of a fluid sandy sediment layer over a rocky semi-infinite sub-bottom as described in Table 1 was adopted [10].

2.1.3 Water column properties

Water column includes physical properties, such as temperature and salinity, that can be used to deduce the water column sound speed profile (SSP). The physical properties of the target area were obtained for the months of January and June 2019 through the Copernicus - CMEMS database [2]. These two periods were chosen as representative of the two extreme cases of the typical evolution through the whole year.

[1] www.gebco.net
[2] https://marine.copernicus.eu/

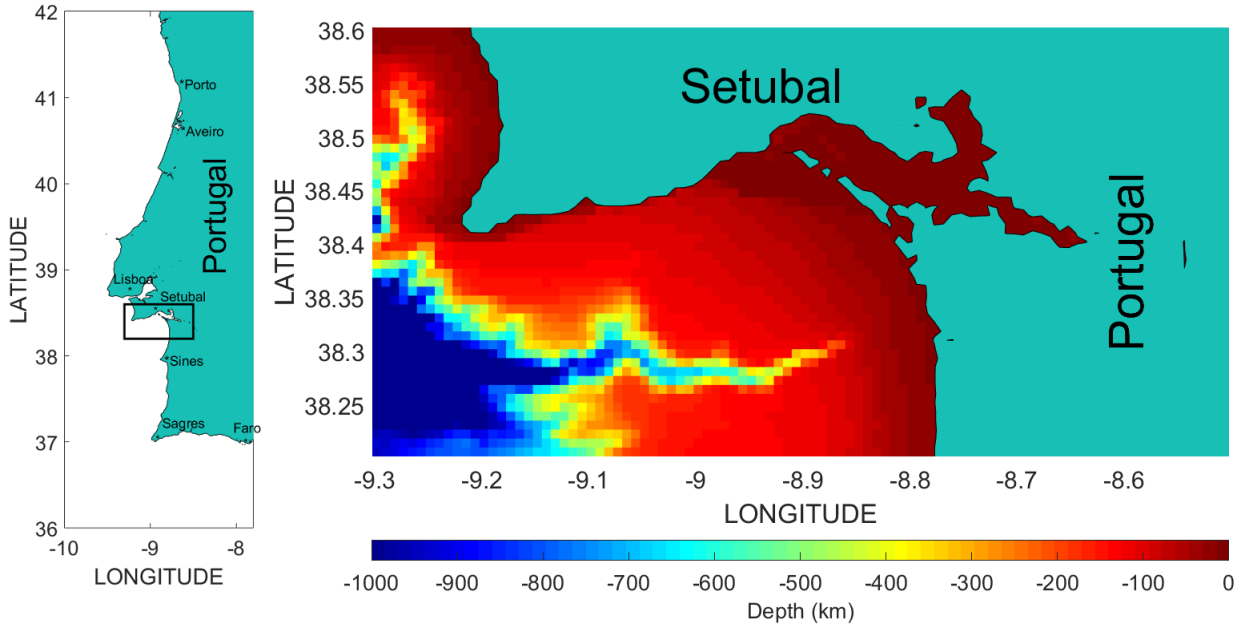

Figure 3: Bathymetry as extracted from the GEBCO database for continental Portugal (left) and the study area detail (right) [9].

Table 1: Assumed seabed parameters (adapted from [10]).

Model Parameter (units)	**Value**
Sediment speed (m/s)	1650
Sediment density (g/cm^3)	1.9
Sediment attenuation (dB/λ)	0.8
Sediment thickness (m)	10
Sub-bottom speed (m/s)	1800
Sub-bottom density (g/cm^3)	2.8
Sub-bottom attenuation (dB/λ)	0.2

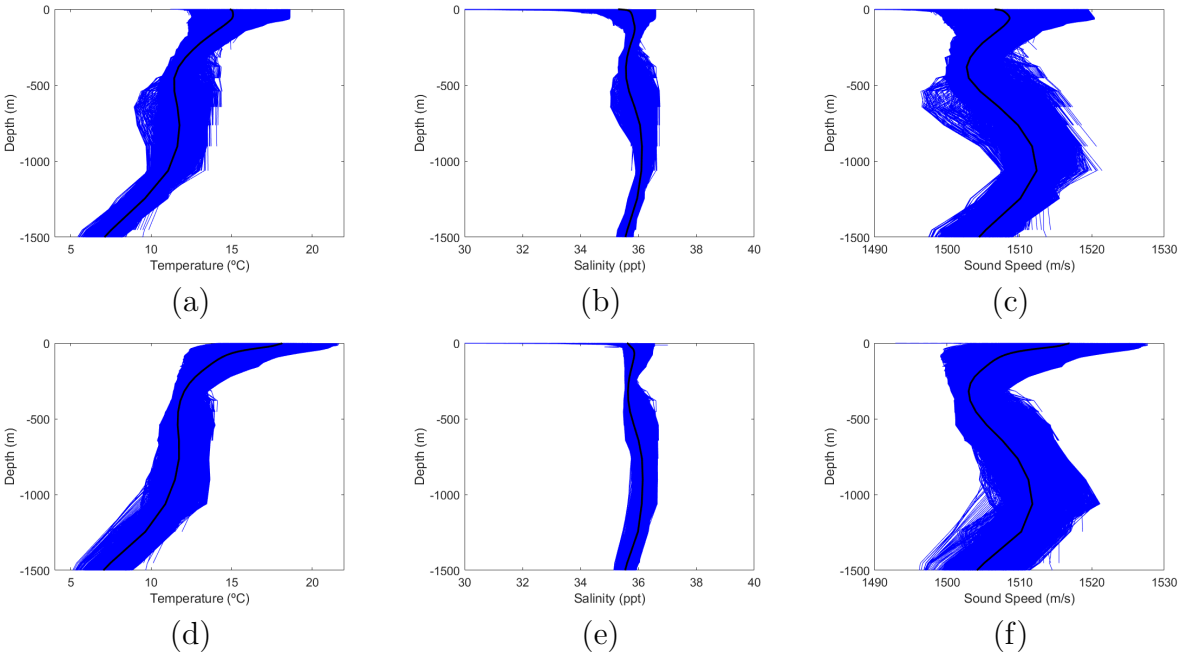

Figure 4: Temperature ((a) and (d)), salinity ((b) and (e)) and sound speed profiles ((d) and (f)) variation for January (top figures) and June 2019 (bottom figures). Note that black lines represent the mean profile of each variable. (Source: CMEMS-Copernicus Marine Service).

Fig. 4 shows the superposition of profiles for the complete area and for the full month of January (upper row) and June 2019 (lower row), for temperature ((a) and (d)), salinity ((b) and (e)) and calculated sound speed ((c) and (f)). For each data set the black line represents the mean profile. As expected, it was observed that temperatures in January are typically lower than in June. A 50 m thick mixed layer is observed for the month of January, followed by a deep gradient until 500 m depth both in January and in June. Salinity shows a similar behavior between January and June (see plots (b) and (d)), with however higher variations in the mid water column in January then in June, with typical values between 35 and 37 parts per thousand (ppt). The sound speed profile was estimated using the nine-term Mackenzie equation, resulting in plots (c) and (f) for January and June, respectively.

As expected, the sound speed profiles of January and June follow, approximately, the same shape as the temperature plots of the respective months. It is also noted that the sound speed in the deeper area is potentially a double minima profile, which is a common feature in this region, due to the warm water sipping through Gibraltar and heading north along the Iberian coast. Since acoustic propagation is very sound speed dependent, it is expected that those differences may have an impact in the propagation of seismic noise, and consequently in the potential harmful effects on marine species on the study area.

2.1.4 Biology of the area

The entire coast of Portugal is known to be a rich ecosystem in terms of marine biodiversity. As an example, Fig. 5 shows the cumulative sightings of cetaceans per unit area of 2x2 km since 2005 obtained by SPEA-the Portuguese Society for the Study of Birds (left) and for 2019-20 by the whale watching company SeaEo (SEO) for the area of Setúbal (right). Fig. 6 shows a series of estimated animal densities based on species records for European Seabass (a), small spotted catshark (b) and blue mussel (c) as examples. The Portuguese coast is in fact known to favour ecosystem richness [8] and cetaceans' occurrence is one of the most studied aspect as well as one of the highlights of the coast. Their presence makes the coast a great spot for sightings activities such as the Whale Watching touristic activity Furthermore, the economy of this area is highly based on fishery, which is one of the major economic entrance of the country [11]. Effectively, apart from cetaceans, records of other marine species' cover an important variety of groups: from fishes to marine invertebrates and sea turtles (see Figures 19, 20 and 21 in the appendix B). The central region of the country, including the Setúbal area, presents high densities of various species, which makes it a very interesting spot of biodiversity (see Fig. 6). In addition, some of these species have been shown to be sensitive to anthropogenic noise.

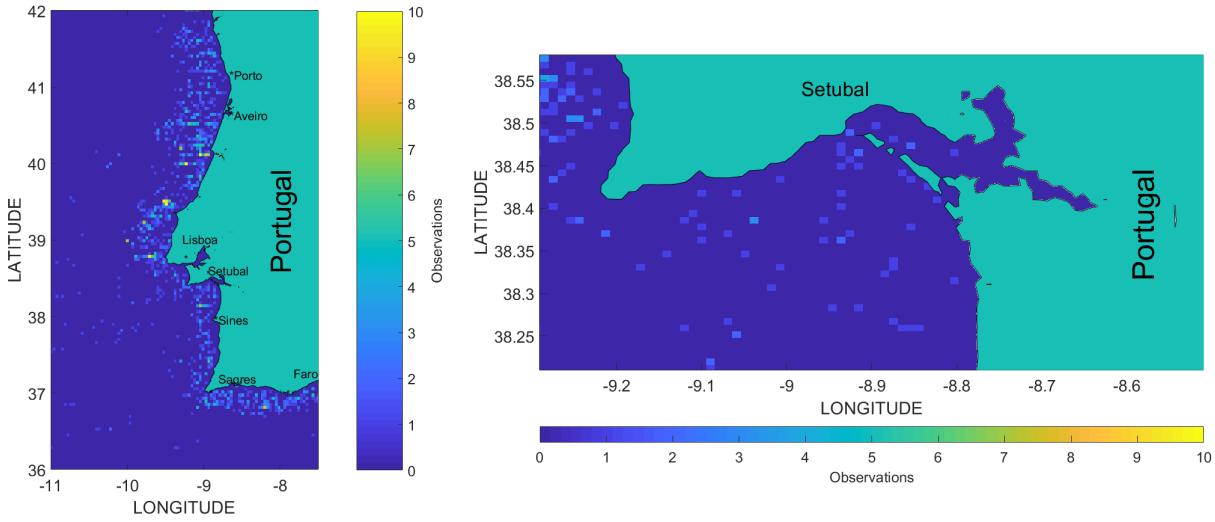

Figure 5: Cetacean cumulative sightings per unit area of 1 x 1 km by SPEA in the period 2005-2020 (left) and by SeaEO for 2019-20 (right).

As a representative of cetaceans' group, we chose the common dolphin (*Delphinus delphis*) since it is one of the most sighted species in the Portuguese coast and also because it was the species with the most available data allowing for the generation of robust models, as described in section 2.3.

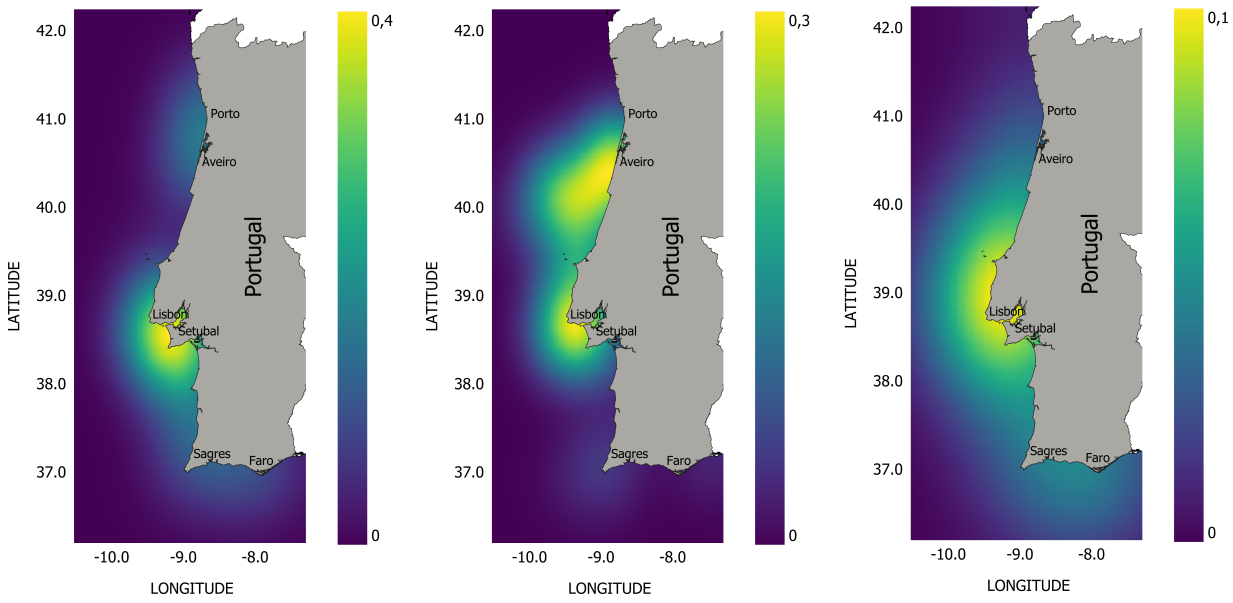

(a) (b) (c)

Figure 6: Animal densities based on species' records for: European seabass (*Dicentrarchus labrax*) (a), small spotted catshark (*Scyliorhinus canicula*) (b) and blue mussel (*Mytilus edulis*) (c).

2.2 Seismic survey modeling

Designing a tool for modeling a seismic survey and its noise emission is a complex task which requires a variety of inputs. The methodology for study area discretization and modeling is described in section 2.2.1, follows in section 2.2.2 the seismic source specification that is used as reference for modeling and finally the computation steps for calculating the acoustic field distribution in section 2.2.3.

2.2.1 Area discretization for modeling purposes

A seismic survey is set to cover a given spatial area. Seismic surveying setup depends on a number of parameters such as water depth, required bottom penetration and resolution, the source firing sequence, ship speed, etc. Once those parameters are set, the total required time for area coverage can be calculated. For area discretization and noise modeling setup of the Setúbal test case, the following parameters were set:

- **area coordinates**: our test case focused on a relatively small rectangular area of 50 km^2 delimited by the following coordinates: longitude -8.92º and -8.87º and latitude 38.34º and 38.42º with a spatial resolution of 1 km x 1 km as shown in Fig. 7. The water depth of the surveying area varies from 30 to 100 m depth which is appropriate for the installation of offshore wind farms;

- **movement pattern**: there is a wide choice of patterns to fit specific environmental requirements. In our test case a traditional lawn-mower pattern is used, giving rise to a regular set of emissions along the area.

- **seismic source depth**: important for bottom imaging, and for introducing in the numerical propagation model, a 1 m depth was chosen for our case.
- **firing interval**: a 5 s interval was chosen for our example;
- **ship speed**: it should be related to the firing interval but a typical value is 5 knot, which gives a firing spacing of $\approx$ 15 m.
- **time resolution**: for sound pressure level was set to 10 min.
- **total duration**: a total duration of one month.

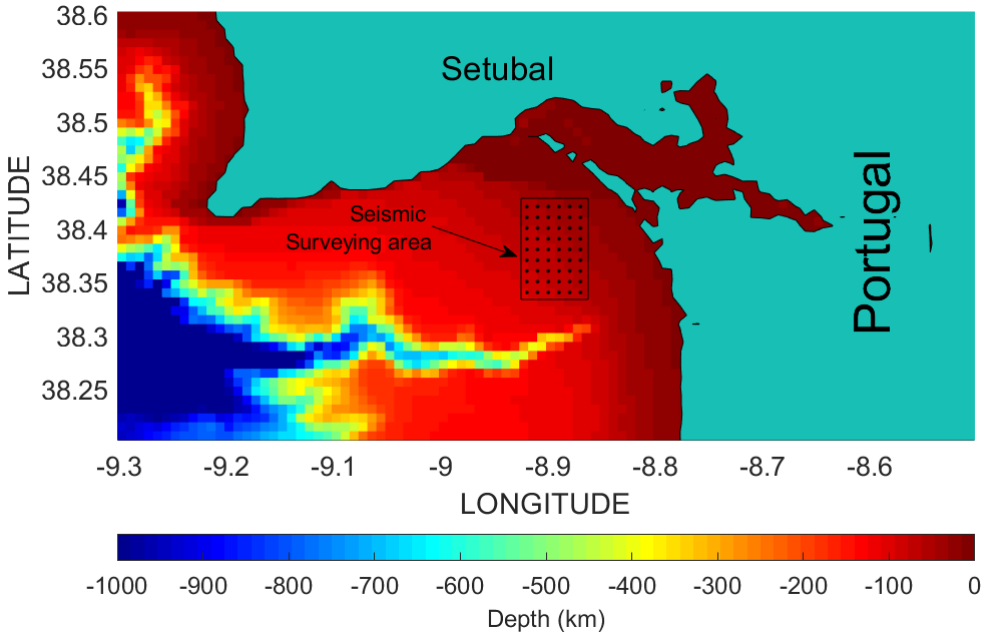

Figure 7: Seismic surveying firing pattern and selected area: rectangular box with dots.

2.2.2 Seismic source selection and specifications

One important required parameter is the choice of the seismic source. In fact this choice is a mix between practical considerations such as hardware availability, cost, etc, and survey requirements such as pulse energy and imaging resolution.

There is a wide variety of seismic sources being used in surveys among which we can highlight: air-guns, sleeve-guns, water-guns, boomers and sparkers. These seismic sources essentially differ in their operating frequency ranges and source levels [12–14]. Table 2 gives a list of the most common type of seismic sources, with their operating frequency band and source level range. As previously mentioned air-guns are used since 1960 and are probably the most well known seismic source since they are largely used in oil and gas exploration around the globe [12]. It consists of one or more pneumatic chambers that are pressurized with air at very high pressures, from 14 to 21 MPa, and when the air gun is fired, the compressed air is released in the water column producing an acoustic

pulse [13]. Sleeve and Water guns have a very similar architecture varying only in the chamber design and expelled "material" respectively.

Table 2: Specifications of typical seismic source types [12].

Seismic Source	**Operating Frequency (Hz)**	**Source Level (dB)**
Boomer	400 - 10000	220 - 222
Sparker	30 - 5000	216 - 226
AirGun	100 - 1000	231 - 260
Sleeve Gun	50 - 1000	230 - 260
WaterGun	20 - 500	200 - 205

Normally, seismic surveying involves an array of individual air guns with different sizes/volumes which are synchronized to create an optimal shock wave with a minimum reverberation. The Sleeve-gun design follows approximately the same principle as the air-gun although it has been engineered with several membrane sleeves each of which fitted around a mixing/firing chamber that releases an explosion when the mixture of oxygen and propane is ignited. This makes it better suited for shallow water. The last of the "guns", the water-gun has been developed in order to reduce some of the deleterious effects of ghosting and reverberation associated with air-guns, however less repeatable and less practical then the former ones. The principle behind water-guns is again similar to the air gun, however, instead of expelling high-pressured air, this source expels a fixed volume of water, forming a cavitation pocket that implodes and creates a seismic pulse [12].

Contrary to the previous three sources, boomers and sparkers are considered light seismic sources due to their "high frequency" characteristics and were specially designed for experiments in shallow coastal areas, that require less energy and higher bottom resolution. Boomers store energy in capacitors, that discharge through a flat spiral coil. A copper plate adjacent to the coil flexes away from the coil as the capacitors are discharged. This flexing is transmitted into the water as the seismic pulse [13]. Sparkers are high-resolution seismic sources that operate by sudden discharge (spark) of a high-voltage electrical current between electrodes. Modern sparker systems use several electrodes, which produce a seismic energy pulse typically between 300 and 20000 J [12]. They are widely used for high-resolution seismic studies, generally for site survey purposes to map shallow stratigraphy, as well as active tectonism in continental margins, and geo-hazards before drilling. Sparker sources have become particularly desirable due to their convenience and reliability [12, 14].

For our test case, a sparker source was selected, that is well adapted to the environmental characteristics of the area. During the H2020 project WiMUST[3] a Geo-Source 200 sparker[4] was experimentally tested in the port of Sines, approximately 50 km south of our study area. The objective of that test was to obtain a direct in field measurement of the source pulse. The source was positioned at the nominal depth of 0.5 m and set to transmit at low level of 300 J. The recording was performed 15 m away at various depths with the results shown in Fig.8 for the waveform (a) and the power spectrum (b). The time waveform looks quite similar for the various depths and the frequency content in-

[3]WiMUST - Widely scalable Mobile Underwater Sensor Technology

[4]developed and commercialized by GEO Marine Survey Systems, Netherlands.

creases sharply from 50 to 500 Hz and then extends at maximum level up to 2 kHz; a high signal level holds up to 5 kHz [15].

According to the manufacturer data sheet this sparker has two arrays of 100 electrode tips each, and may operate at various levels up to 1000 J reaching a source level of 223 dB at 1 m depth. This source is suitable for water depths from 2 to 500 m, with a penetration of 200-300 ms (*e.g.* 300 to 500 m) below the seabed depending on the geology.

Although the range of audible frequencies of cetaceans may extend well beyond 1000 Hz, in this study and in order to maintain the noise calculation computational burden manageable, only the frequency range 300-1000 Hz was used.

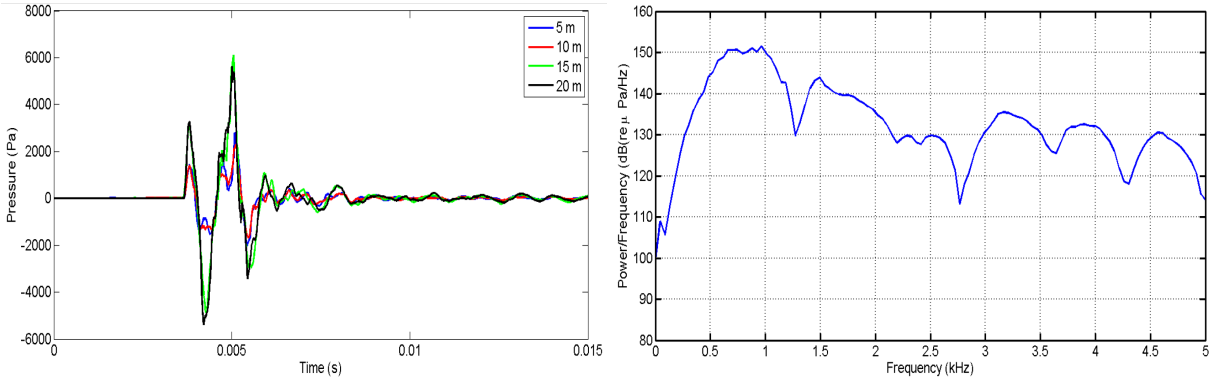

(a) (b)

Figure 8: Sparker test data acquired during the WiMUST 2017 sea trial: time waveform recorded at four different depths from 5 to 20 m (a) and its power spectral density (b).

The seismic source used during the test case was parameterized for noise modeling purposes, with the values shown in Table 3.

Table 3: Geo-Source 200 sparker source parameter settings.

Parameter [unit]	**Value**
Depth [m]	1
Power [J]	1000
Source level [dB // μPa]	223
Frequency [Hz]	300-1000
Duty cycle [s]	1/5

2.2.3 Noise field computation

The noise distribution was calculated in two steps taking into account the pulse data of the sparker source described in the previous section:

- estimation of the acoustic transmission loss (TL);
- conversion of the range-azimuth discs to latitude, longitude and depth and their sum at a given time to obtain the actual SPL in the area.

In the first step the normal mode propagation model KRAKEN [16] was used, taking as inputs the environmental description combining water column, bathymetry and seafloor parameters as described above. This was used to calculate the TL from each source position to every point in a spatial grid defined by a disc of variable range R_r and azimuth θ_r for a fixed depth. The received root-mean-square (rms) power spectral density $Y_n(R_r, \theta_r)$ is given by

$$Y_n(R_r, \theta_r) = \sqrt{\sum_{k=1}^{K} |S(\omega_k)|^2 |\mathrm{TL}_n(\omega_k, R_r, \theta_r)|^2}, \tag{1}$$

where the summation is performed over a given discrete number of frequencies K, at which the TL (in rms power units) is calculated, and where $S(\omega_k)$ is the power spectrum of the nth source. In a second step, SPL is obtained as the range-azimuth discs of each individual source are converted to latitude-longitude-depth coordinates, and then summed over all N sources.

$$\mathrm{SPL}(lat, lon, depth) = 10 \log_{10} \sum_{n=1}^{N} |Y_n(lat, lon, depth)|^2. \tag{2}$$

As previously described by Duarte et al. [17], one way to evaluate the sound pressure level resulting from seismic surveys is to evaluate individually the effect of the sound source at each specific location. Usually, noise maps deal with continuous noise in 1/3-octave bands, however the assumptions for 1/3-octave bands may not be valid when dealing with impulsive noise that is emitted only at given time intervals. Considering that seismic exploration deals with a succession of periodic pulses at a given time rate, the concept of sound exposure level (SEL) that allows to include transmission time will be used. In a T_0=5 s cycle only $T = 1$ s is active, therefore using the usual definition of SEL (recalled in appendix A) as:

$$\mathrm{SEL} = \mathrm{SPL} + 10 \log_{10} T/T_0 \tag{3}$$

gives a correction factor of approximately -7 dB relative to SPL. However this does not takes into account the time spreading nature of the acoustic channel, which may make the short emitted pulse look much longer at the receiver. In fact the quantity of interest will be the emitted and specially the received energy, rather than the frequency band power based on 1/3-octave bands only, as normally used for SPL definition. In order to better grasp the difference, a test was performed according to the following steps:

- two points A and B, representing source and receiver, spaced 2 km apart were selected in the study area. KRAKEN was lunched for all frequencies between 300 and 1000 Hz in order to estimate the channel impulse response (CIR);
- the input signal was convolved with the CIR to obtain the received signal;
- the SEL was calculated for a duration of 10 min with a duty cycle of one pulse every 5 s;
- the obtained SEL was then compared with the SPL obtained considering 1/3-octave band levels, and a 4 dB correction factor was determined, that was subsequently used in the simulations.

2.3 Habitat suitability modeling

The Habitat Suitability maps were developed considering only the common dolphin population and taking into account species observations and environmental characteristics of the area. The adopted methodology is described in the following sections. Habitat Suitability maps were created from species observations and environmental layers with the MaxEnt software [18].

2.3.1 Data collection

Animal occurrences were obtained from two different types of opportunity platforms over a period of fifteen years (from 2005 to 2020). The first source of observation records comes from linear routes performed by the Portuguese Society for the Study of Birds (SPEA) dataset (as shown in the cumulative map of Fig. 9 (a)) carried out with the European Seabirds At Sea (ESAS) method[5] along the whole coast of Portugal to a maximum distance of 75 km from the coastline. SPEA dataset spans the period from 2005 to 2020, with records equally distributed along the year.

The other two sources of occurrence records were whale-watching companies: "SeaEo tours" (SeaEO) in Setúbal Bay and "MarIlimitado" (MI), in Sagres, shown in maps of Fig. 9 (b) and (c), respectively, with a smaller coverage then the SPEA dataset. The described datasets are summarized in Table 4.

Table 4: Animal occurrences' datasets characteristics.

Observations' source	Code	Region	Coordinates Lon x Lat	Period of time	Background points creation method
SPEA	SPEA	Portuguese coast	[-10.5 -7.5]x[36 42.5]	2005-2020	Using the transects of boat trips for all the species
SeaEO tours	SeaEO	Setúbal	[-9.6 -8.7]x[38.3 38.8]	2019-2020	Minimum Sampled Area (MSA)
MarIlimitado	MI	Sagres	[-9.3 -8.5]x[36.7 37.2]	2005-2020	Minimum Sampled Area (MSA)

SeaEO tours observations cover a two year period, 2019-2020, and they were collected whole year round. Instead, Mar Ilimitado dataset covers a much wider period, from 2005 to 2020, but with records mostly concentrated between the months of April and October. The selected spatial resolution was of 2x2 km since it agrees with the resolution of the sampled area, it agrees with the resolution of the environmental layers and it fits with the ecology of the selected species.

2.3.2 Environmental variables used in HS modeling

Five environmental variables were selected as potential explanatory variables to calibrate models of habitat suitability for the common dolphin (see Table 5).

Terrain variables, depth, and seabed slope were derived from a digital elevation model (DEM) layer downloaded from NOAA (ETOPO 1 Global Relief Model[6]). Depth was directly read from the DEM and the seabed slope was calculated using QGIS[7] as the

[5]https://jncc.gov.uk/our-work/monitoring-seabirds-at-sea/

[6]`https://maps.ngdc.noaa.gov/viewers/bathymetry/?layers=dem`

[7]version QGIS 3.18, Zurich available at: www.qgis.org/

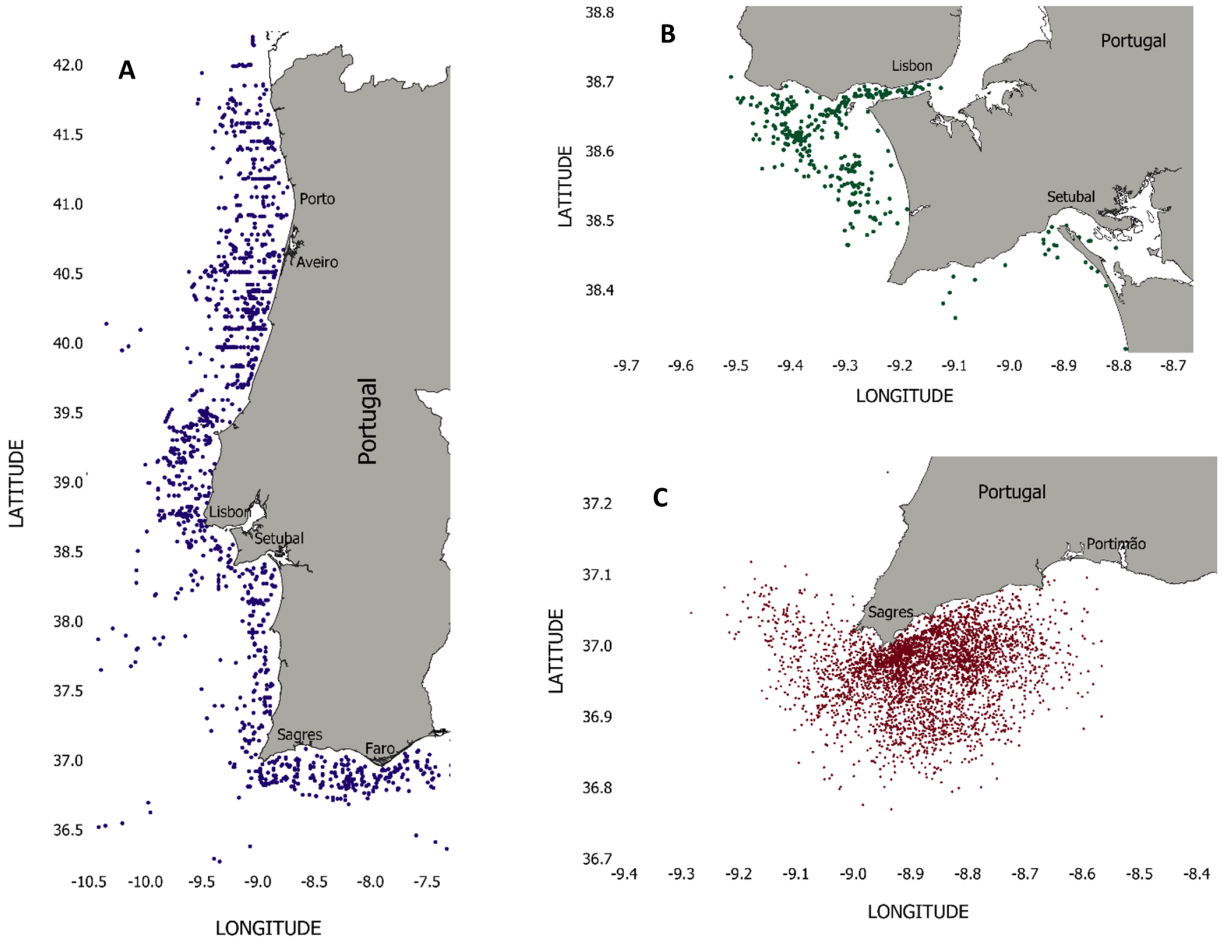

Figure 9: Cumulative observation records spatial distribution of marine mammals from: a) SPEA dataset; b) SeaEO dataset; and c) MI dataset.

gradient of maximum change in depth for each grid cell, ranging from 0^{o} to 90^{o}. These two physical variables, are known to directly influence the distribution of cetaceans.

The three oceanographic variables, Sea Surface Temperature (SST), Chlorophyll-a (as proxy for primary productivity) and Standard deviation of the Chlorophyll, were extracted from the Copernicus Marine System platform with daily temporal resolution from June 2005 until June 2020. Data were then pulled together into a temporal resolution of 8 days, which is the resolution used for the previously described model input data. See the complete description in Table 5.

The surface chlorophyll (Chl-a) data was obtained from the ESA Ocean Color CCI Remote Sensing Reflectance data (by merging layers from SeaWiFS, MODISAqua, MERIS, and VIIRS sensors and realigning the spectra to that of the SeaWiFS sensor) using the regional OC5CCI chlorophyll algorithm. Moreover, the Sea Surface Temperature (SST) was obtained from the Group for High-Resolution Sea Surface Temperature (GHRSST), a global, gap-free, gridded, daily 1 km dataset created by merging multiple Level-2 satellite SST datasets. Layers were then scaled to the specific temporal and spatial resolution.

To detect the presence of collinearity among environmental predictor variables, we applied a variance inflation factor (VIF) approach implemented in R Studio [19]. None of the selected environmental layers had collinearity issues. Collinearity is the linear dependence among environmental predictor variables and it is known to be a challenging issue in ecological niche modeling [20].

All environmental layers were processed to have the same geographic extent along Portugal mainland coastline until a maximum of 75 km from the coast, with the same projection system (World geodetic System [WGS] 1984 zone UTM 29N), and cell size of 2x2 km, then converted to an ASCII raster grid format using QGIS 3.18.

Table 5: Selected environmental variables.

Environmental Variable	ACR	UNIT	Source	Modifications
Depth	DEPTH	m	NOAA, ETOPO 1 Global Relief Model	Resampled to the selected resolution and extent
Slope	SLOPE	°	Calculated on QGIS3.18	Resampled to the selected resolution and extent
Sea Surface Temperature	SST	K	Copernicus Marine System	Scaled to the selected temporal and spatial resolution
Chlorophyll-a	CHL	mg.m-3	Copernicus Marine System	Scaled to the selected temporal and spatial resolution
Chlorophyll-a Standard Deviation	SD_CHL	mg.m-3	Calculated from the CHL layer	Scaled to the selected temporal and spatial resolution

2.3.3 Sampling bias correction

One of the biggest issues with data collected on platforms of opportunity, especially on whale-watching vessels, is that it may have several biases which have to be taken into account in the creation of the models. In particular, the touristic nature of this activity often generates sampling effort bias. For instance, it is quite common that the same group of animals is sighted more than once in a similar location, both in space and time. This can cause autocorrelation problems in adjacent grids. Hence, a filtering approach was

applied to remove potentially related sightings. A spatial thinning process was applied to all the sightings, for temporal grouping of 8 days, with the purpose of filtering observations concentrated in the same small spatial area. In practice, the thinning process removes "the fewest records necessary to substantially reduce the effects of sampling bias, while simultaneously retaining the greatest amount of useful information" [21]. In addition, occurrences were also resampled to one occurrence per pixel for each temporal grouping (8 days).

Sampling effort bias are one of the major problems within the construction of Species Distribution Modeling (SDM). Potential sampling effort bias in our study area are of two kinds: a) due to a possible lack of records in an area of potential priority resulting from the absence of survey effort in that area and b) due to the fact that records in regions where the sampling effort was high might over represent the presence of a species.

To overcome the different biases from the occurrences datasets, a target-background approach was used. Accounting for sampling bias is the greatest challenge facing presence-only and presence-background species distribution models. When no sampling correction is applied to the model, there is the risk to map sampling effort rather than the underlying habitat suitability. When using a target-background method, the selection of background points is manipulated to increase the contribution of environmental variation from potentially high sampled areas [22].

Two different target-background methods were applied according to the different nature of the selected dataset:

- **SPEA dataset:** to create the background data and to have a measure of the potential sampled area, transects between all the points with records for all species of birds and cetaceans (not only the target ones) over a period of 8 days were considered;
- **Whale Watching (WW) dataset:** due to the opportunistic nature of the sampling effort, a Minimum Sampled Area (MSA) approach was applied, as used in Fernandez et al. (2017) [23]. All the sightings for each specific temporal scale and for all species (again including the non-target ones) were pulled together using a Minimum Convex Polygon, adding a 1 km buffer. Grids intersecting the polygon were considered as potentially sampled areas, therefore classified as background.

The total amount of effort per temporal unit (8-days) was considered using the number of sea trips performed on a specific period. Occurrences and the selected background grids from both datasets were put together to proceed with the MaxEnt analysis. For each analysis, random background datasets (n = 10,000) were generated.

2.3.4 MaxEnt modeling

Maximum Entropy modeling, as described in [18] was used to obtain habitat suitability maps for the common dolphin along the Portuguese coast. The HS maps resulting from this modeling, for the selected months of January and June, were cropped for the detailed study area of Setúbal.

Maximum entropy models (Maxent models) belong to the family of the Ecological Niche Models (or Species Distribution Models). The inputs are the species records and the

selected environmental variables. These variables should have a temporal correspondence with occurrences data, and they should affect the species' distribution at the pertinent temporal and spatial scales. The principle of maximum entropy is employed to relate observations data to environmental variables. The results of such models are Habitat Suitability maps that give an estimate of the species' ecological niche and the potential geographical distribution [18]. Habitat can be defined as "an area with a combination of resources and environmental conditions that promotes occupancy by a given species (or population) and allows those individuals to survive and reproduce" [24]. Suitability indicates the quality of these conditions and resources.

Another output of these models, is the importance that each environmental variable has in the habitat suitability of the species, as shown in the data flow diagram of Fig. 10.

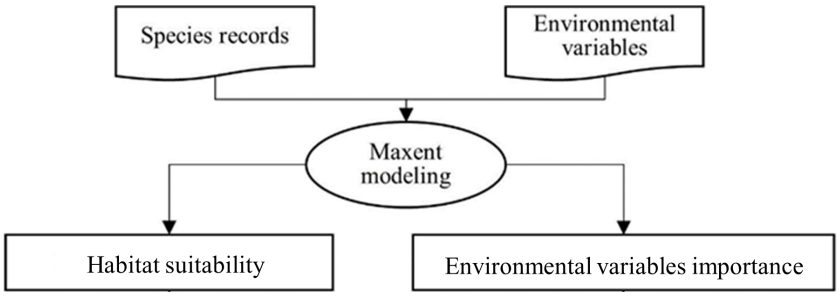

Figure 10: Methodological framework of Maxent modeling (adapted from [25]).

Maxent models were chosen for this study among other methods because:

- only few input data (species records and environmental variables) are required;
- environmental variables can be continuous or categorical;
- efficient deterministic algorithms that are guaranteed to converge to the optimal (in the maximum entropy sense) probability distribution are employed;
- the Maxent probability distribution has a concise mathematical definition and it is thus amenable to analysis;
- it allows to address the issue of sampling bias formally;
- being a generative approach, it may give better predictions for small data amounts, such as those available in this study, than other concurrent approaches

Maximum entropy models have strong similarities to some other existing Environmental Niche Models (ENM), such as generalized linear models (GLMs) and generalized additive models (GAMs). However, those are presence-absence models, where absence data are required, while Maxent is mostly used for presence-only data as that of our data sets [18].

2.4 Risk assessment methodology

In the underwater acoustic domain, risk may be defined as quote "the possibility of occurrence of an harmful effect that can result in a severe or mild injuries in marine

species due to the anthropogenic noise sources", end quote [26–29]. For this reason, it is important to estimate risk areas resulting from human activities in order to stimulate the development of measures at a governmental level to protect species.

2.4.1 The classical approach

The definition of risk assessment is not consensual in the scientific community. Verling et al. [28] state that risk is defined by $Risk = Likelihood$ X $Consequence$ where $Likelihood$ defines the points in space where risk occurs, or more exactly, quantifies how likely it is that a given sound pressure "overlaps" the ecosystem element related to the presence of that particular species. The $Consequence$ defines what exactly might happen in case of some $Likelihood$. This definition may appear relatively simple but its assessment requires a number of steps some of which are drawn from legal definitions of current MSFD regulations and others are drawn from data inference [28].

A more pictorial representation of the same issue is shown in figure 2 of Merchant et al. [27]. In this case obtaining the risk map (shown in panel D of figure 2) is a "simple spatial overlaying" of panels B and C of population density and noise pressure map, respectively.

Another classical approach is that proposed by Erbe et al. [30] where noise maps and densities are provided in normalized scales 0 to 1. The authors refer that the risk map is obtained through multiplying species density in the area by the noise distribution and re-normalizing the final result. It is also mentioned that the resulting risk map can not be used for comparison between species, but gives a relatively good assessment of areas at high noise risk for the considered species. In the absence of a better risk assessment methodology the so-called "Erbe method" will be used as the classical approach to assess risk in this study, considering a spatial resolution of 2 km x 2 km which agrees with the spatial resolution in HS models.

Additionally, an important point that should be taken into account when evaluating risk for a particular species is the auditory sensitivity of that species, *i.e.*, the range of frequencies that it can hear/communicate with, which may be represented in the form of an audiogram. Each species has its own audiogram and Erbe *et. al.* [26] summarized several audiograms of the *Delphinidae* family which were used as reference in this report (Fig. 11).

Toothed cetaceans (*odontocetes*), including all dolphins, are generally considered as Medium/ High-Frequency cetaceans (MF and HF cetaceans), since they emit loud echolocation clicks and communicate with high or medium pitched frequency. Sensible frequency ranges normally extend from several Hz to 100 kHz [31]. Seismic source frequency range considered in this study is instead considerably smaller (from 300 to 1000 Hz) compared to the ranges of these HF species. In addition, information concerning common dolphin hearing sensitivity, compared to other Delphinidae, is really scarce and the few available audiograms concerning this species didn't reach frequencies where seismic survey operates [31]. For these reasons, we decided to use audiograms from other dolphins belonging to the Delphinidae family, in order to allow this overlapping between seismic frequencies and species sensitivity to happen. Fig. 11 shows the audiogram of the bottlenose dolphin (Tursiops truncatus) used in this study, since it is the species that presents the major overlapping with seismic frequencies.

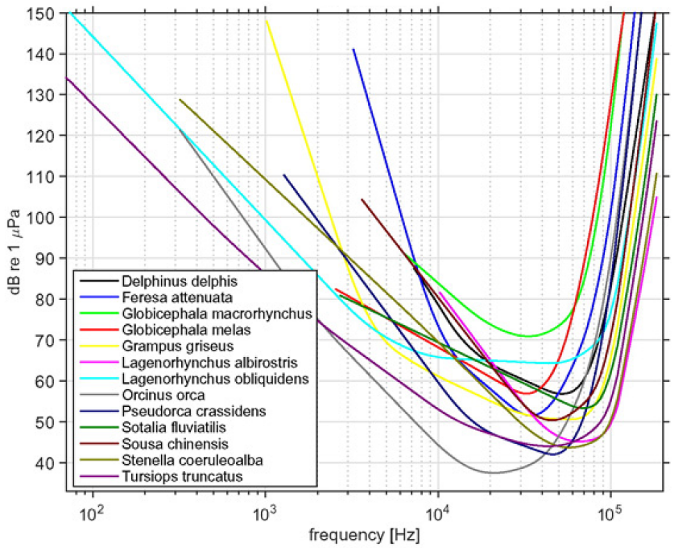

Figure 11: Audiogram levels measured for various species of cetaceans (adapted from [26]).

2.4.2 Alternative Bayes-based approach

An alternative approach for estimating risk areas may be based on the combination of HS and noise resulting from seismic surveying based on the Bayesian inference. The reasoning follows from seeing noise as a random variable B related to animal presence denoted by random variable A, in a given location and time. If variable A may be represented by a prior distribution such as HS, then the conditional density of $B|A$ will be given by the distribution of noise. It follows that the posterior distribution of A, after noise observation, denoted as the random event $A|B$, will be given by the classical Bayes theorem

$$p(a|b) = \frac{p(b|a)}{p(b)} p(a) \tag{4}$$

where $p(\cdot)$ represents probability density function (pdf) and where the denominator is a simple (but important) normalizing factor $p(b) = \int p(b|a)p(a)da$. It is important because it scales the result so it becomes comparable. In (4) a represents animal presence and b noise level. Estimation theory indicates that an estimator that minimizes the Bayesian mean square error is given by the conditional mean of the posterior distribution (after observation), or the mathematical expectation $E[A|B]$ written as

$$\hat{A} = E[A|B] = \int ap(a|b)da. \tag{5}$$

Although the HS index may be assimilated to a probability, the available dataset and time resolution in our test case did not allow to obtain a truthful prior pdf estimate $p(a)$. Therefore (4), and thus the estimator (5), could not be worked out. However, Bayes may be equated exactly for Gaussian densities. In clear, if the prior and the observation densities are both Gaussian, then the posterior is also Gaussian, which simply states the fact that the product of two Gaussian functions is also a Gaussian function.

So, under the Gaussian assumption and ONLY under that assumption, if $A : N(m_A, \sigma_A^2)$ and $B|A : N(m_{B|A}, \sigma_{B|A}^2)$, the posterior density $p(a|b)$ of a random variable $A|B$ is still

$N(m_{A|B}, \sigma^2_{A|B})$ where mean and variance are given by

$$m_{A|B} = \frac{m_A \sigma^2_{B|A} + m_{B|A} \sigma^2_A}{\sigma^2_A + \sigma^2_{B|A}}, \tag{6}$$

and

$$\sigma^2_{A|B} = \sqrt{\frac{\sigma^2_A \sigma^2_{B|A}}{\sigma^2_A + \sigma^2_{B|A}}}. \tag{7}$$

Therefore, if the prior densities on the right hand side of (4) are approximately Gaussian and we know (or can estimate) their means and variances, we can compute the maximum a posterior Bayes estimator (5) using expression (6), and the variance of the resulting distribution is given by (7), which is not the variance of the estimator, but is a measure of performance since it represents the Bayesian mean-square-error, *i.e.*, the smaller the better.

3 Results

The following section presents the results obtained for the Setúbal area test case as: a) noise resulting from a simulated seismic survey, b) the habitat suitability for the common dolphin species and c) the predicted risk assessment for the population of common dolphin resulting from a seismic surveying event.

3.1 Seismic survey modeling

This subsection shows the sound exposure level resulting from seismic surveying prediction models during the months of January and June 2019 Fig. 12 and Fig. 13, respectively. The 1/3 octave band levels between 315 to 1000 Hz in 1/3-octave band levels. The receivers placed at 5, 15, 30, 50, 75 and 100 m depth. The statistical indicators 5, 25, 50 and 75 percentiles were used.

In both, January and June, it was observed that noise propagation is largely influenced by the bathymetry of the area. The signal is significantly attenuated over the entire platform till it reaches its edge. At that point, the signal is dispersed over a much larger water column, so the SPL abruptly falls off. Additionally it was observed that the exposure levels calculated in January are higher and wider extended than the ones presented in June. This fact may be explained by the sound speed profiles of both months which was described in the previous section2.1.3. In both cases, noise generated largely exceeds the typical mean ambient noise, resulting exclusively from wind, of 65-75dB and the noise produced by continuous noise sources as ships (≈120dB according to Soares *et.al.* [10]) and consequently represents a potential harmful impact on species that are sensitive in these frequency bands.

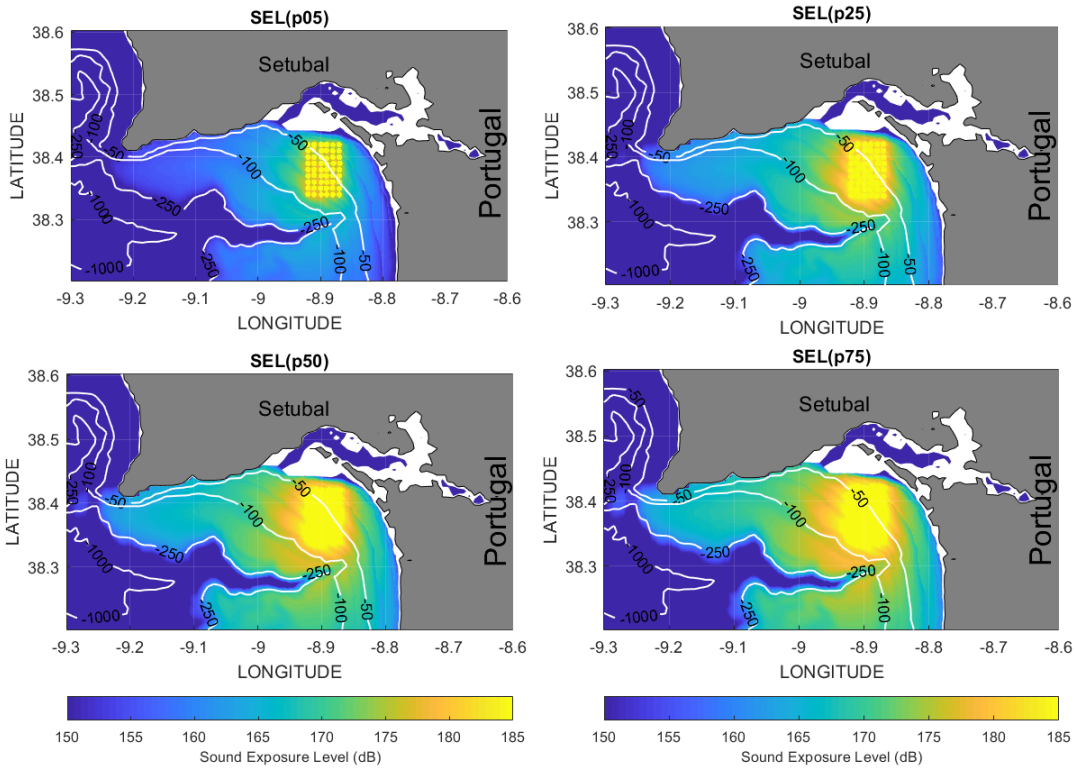

Figure 12: Sound exposure level statistics for the month of January.

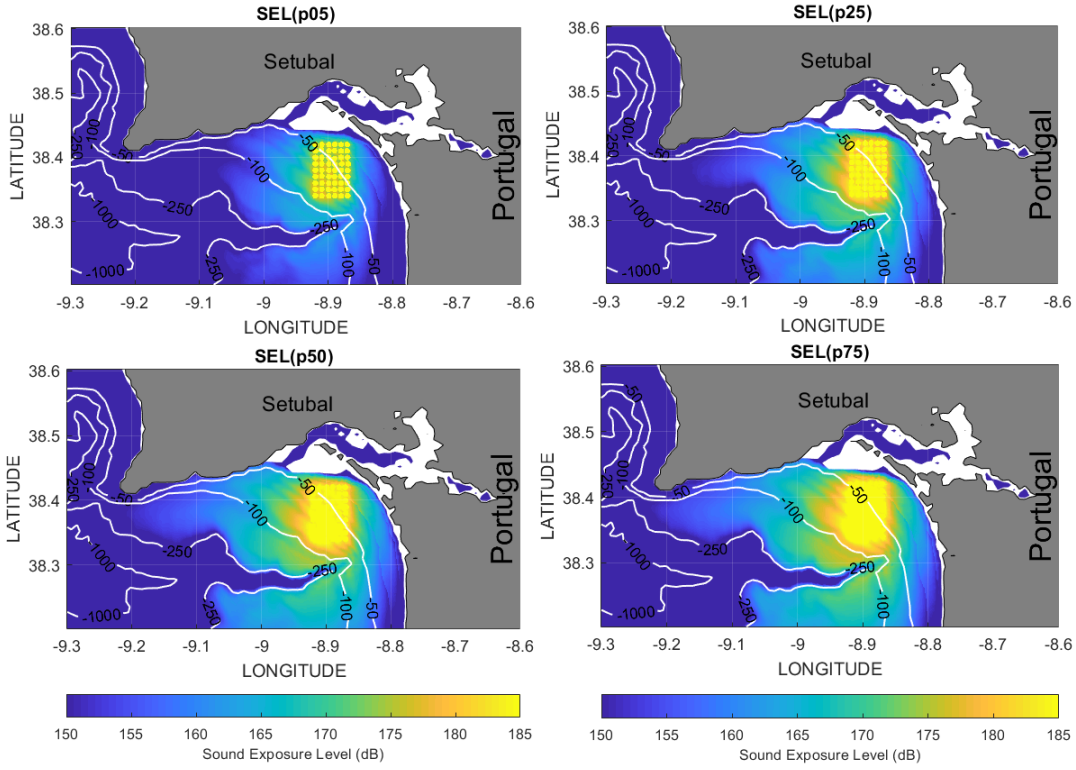

Figure 13: Sound exposure level statistics for the month of June.

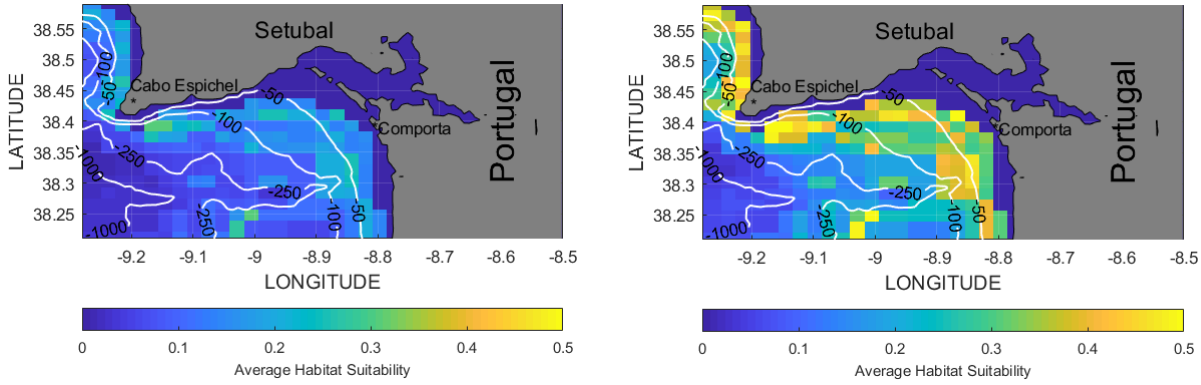

(a) (b)

Figure 14: Common dolphin habitat suitability for the months of a) January and b) June.

3.2 Habitat suitability modeling

Common dolphins are one of the most abundant cetaceans in the North-east (NE) Atlantic and show an important presence along the Portuguese coast, with the region of Setúbal known to be an area with a high number of individuals [32].

It was assumed that for one specific species, habitat suitability can be interpreted as an estimate of the probability of species presence, conditioned on environmental variables [33], indicating the habitat quality for that particular species. Habitat suitability for common dolphin in the area of Setúbal was modeled for the months of January and June shown in Figure 14 (a) and (b) respectively.

The results show that the quality of the habitat for the common dolphin is better in summer season than in winter. However, in both months, the most favorable conditions are around the bathymetric line of 50 m depth in the continental platform and around 100-200 m depth in Cabo Espichel, where the platform shortens. Cabo Espichel and Comporta are the locations where the habitat suitability presents the highest values.

3.3 Risk assessment

The risk assessment results section is divided in two parts, the first one showing the higher and lower risk areas predicted with a classical methodology and the second one obtained using a proposed Bayes-based approach.

3.3.1 Classical risk assessment approach

Fig. 15 shows regions of predicted risk for the community of common dolphins, estimated in the region of Setúbal for the months of January (a) and June 2019 (b), obtained considering the risk assessment methodology described by Erbe *et.al.* [30]. This methodology, defines the risk as the normalization of the multiplication between the noise level map and the habitat suitability, both previously normalized.

It can be observed that January shows lower risk areas than June although the "affected area" has a much larger extension in the month of January than June. In both

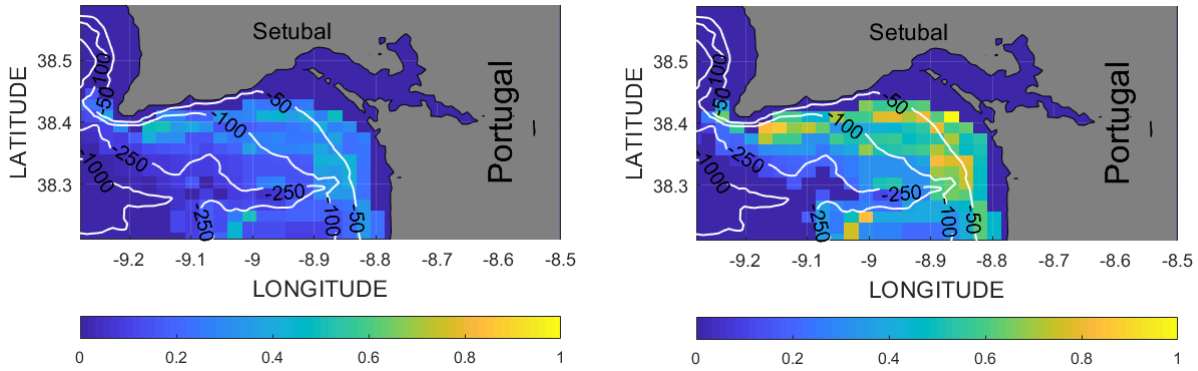

Figure 15: Erbes' method risk assessment results for the common dolphin population for the months of a) January and b) June.

cases it was observed that the highest risk areas are located near the shore, especially till the bathymetric line of 100 m. As it was previously observed, the region near Comporta presented the highest risk levels, which in fact may be due to the highest concentration of dolphins in this area as described in the previous section3.2.

3.3.2 Proposed Bayes-based approach

Fig. 16 shows the risk distribution map using a Bayes-based mean estimator for January and June (a) and (c) and their variances (b) and (d) respectively. The estimated risk maps (Fig. 16 (a) and (c)), look quite coherent with those obtained with the "Erbe method": the spatial distribution of lows and highs follows the same pattern and the overall behaviour between the two months is also similar. This alternative method gives additional information on the variance (Fig. 16 (b) and (d)), which provides an indication of the quality of the estimate. In this case, it points out a better estimate in June than in January.

In order to allow a visual comparison between Bayes' and Erbes' methods it was decided to normalize the results in Fig. 16 (a) and (c) which are shown in Fig.17 (a) and (b) respectively. The comparison corroborates the results obtained with the Erbes' method.

4 Discussion

The present work developed a tool to predict noise levels resulting from a seismic surveying and its impact on marine species. This tool was tested to assess the impact of a seismic survey on the community of common dolphins in the region of Setúbal, Portugal.

The seismic survey modeling results show the expected influence of the bathymetry in the acoustic propagation, attenuating the signal over the entire platform and dissipating it over a much larger water column when it goes beyond the edge of the continental platform.

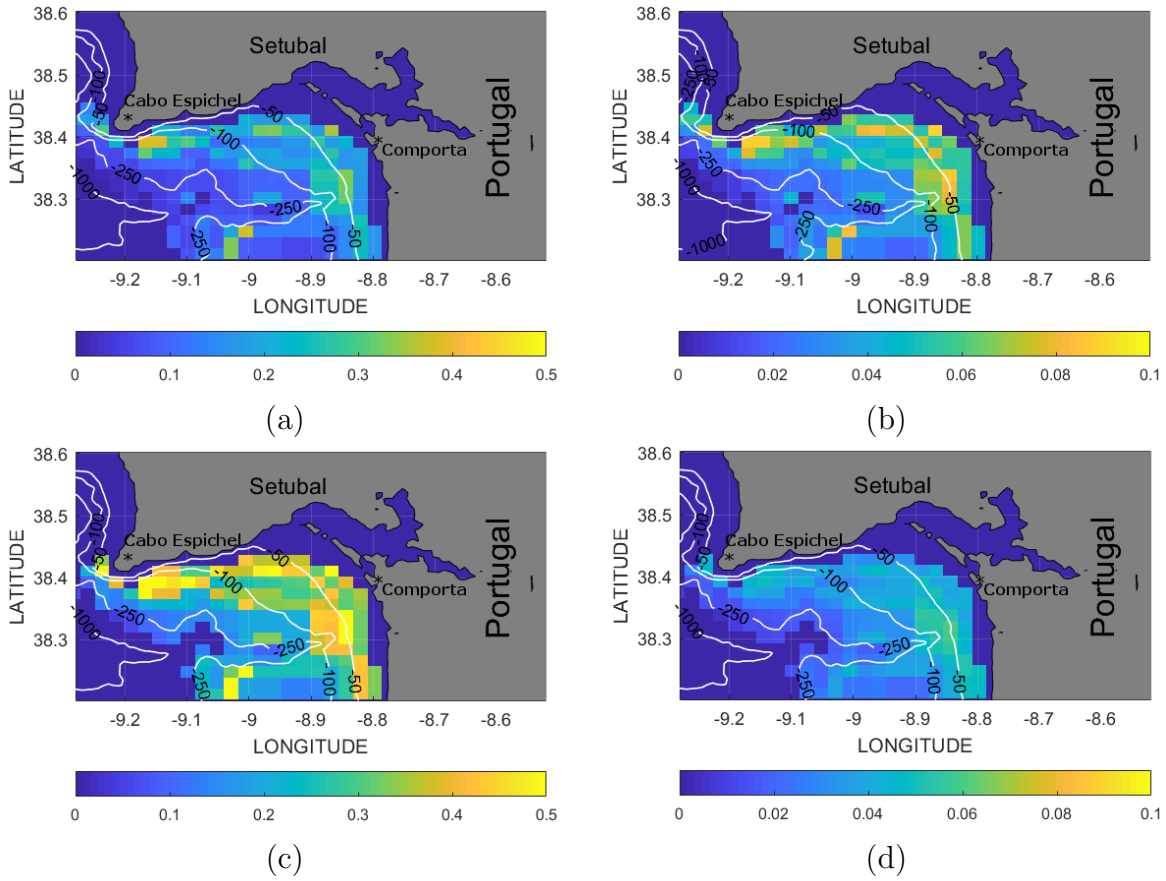

Figure 16: Risk assessment using Bayes-based mean estimator for January (a) and variance (b) and for June (c) and variance (d) (according to eq. 6 and eq. 7 respectively).

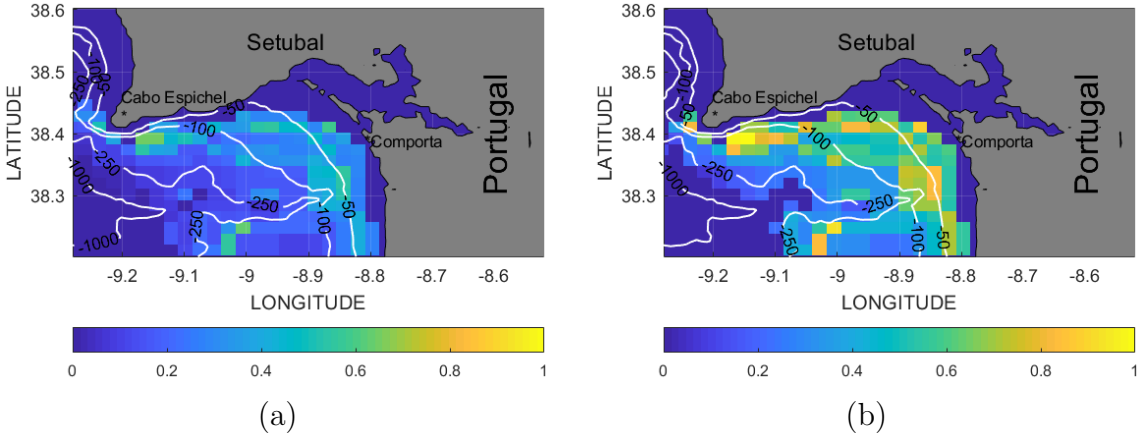

Figure 17: Normalization of the results obtained with Bayes-based methods for January (a) and June (b).

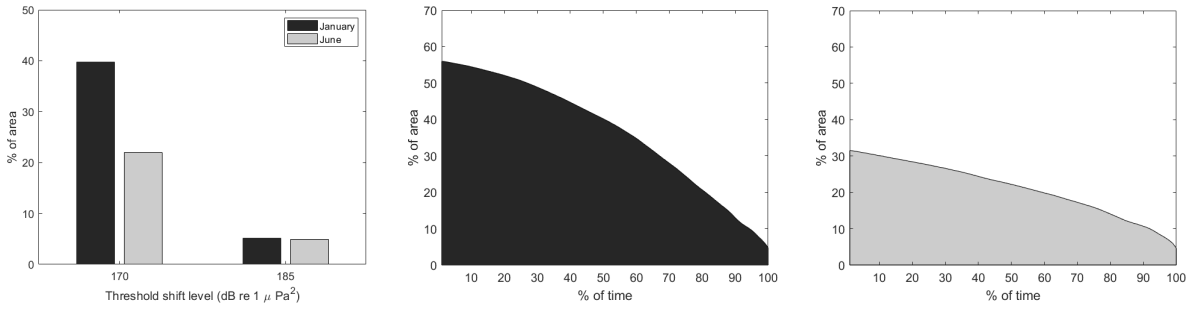

(a) (b) (c)

Figure 18: Temporary and permanent threshold shift for medium frequency marine mammals: a) TTS and PTS exceedance area for January and June, b) and c) TTS exceedance for a percentage of time and area for the month of January and June respectively.

Additionally, the results showed that the noise resulting from a seismic exploration in January extends over a larger area than in June. This fact is related with the temperature of the water which influence the sound speed profile of the water column and consequently the acoustic propagation.

One of the potential effects of noise on animals is the impairment of hearing. This implies short (temporary) or long-term (permanent) changes in hearing sensitivity. These effects can have crucial consequences on the fitness and survival of the animal. In fact, it may affect the capacity of the animal to seek and capture its preys and in the avoidance of predators. It also causes communication issues between individuals which can consequently affect the survival, and the reproductive success. These effects can finally impact an entire population's parameters with consequences such as reduction in population size, reduction in genetic diversity and reduction in total biomass, which could potentially lead to a decline in the population viability and an increase in the extinction rate. Temporary changes in hearing sensitivity are defined as Temporary Threshold Shift (TTS), while the permanent ones as Permanent Threshold Shift (PTS).

Numeric thresholds for predicting auditory effects on marine mammals exposed to a seismic survey were derived from TTS (Temporary Threshold Shift) and PTS (Permanent Threshold Shift) values highlighted by Finneran [34] for the group of mid-frequency cetaceans (group MF: delphinids, beaked whales, sperm whales) to which the common dolphin belongs. The numeric TTS threshold for mid-frequency cetaceans corresponds to 170 dB, while the value of PTS to 185 dB.

Fig. 18 (a) shows the TTS and PTS for a percentage of area which was calculated using the SEL percentile 50 presented in Fig. 12 and Fig. 13 for the months of January and June respectively. Then, Fig. 18 (b) and Fig. 18 (c) show the TTS for a percentage of area over a percentage of time for both months. From the results of Fig. 18 it is evident a seasonality in the exceedance of the TTS levels since in the first case, 170 dB threshold is exceeded in $\approx$ 40% of the area in January and $\approx$ 22% of the area in June. On the contrary this seasonality is not observed when considering the PTS since in both cases 185 dB are exceeded in approximately in the same % of area ($\approx$ 5%). In general, TTS threshold is exceeded in wide areas and for important percentages of time.

On the other hand, the results of the habitat suitability show that in both cases, the

higher habitat quality area follows the coast line configuration, especially considering the bathymetric line of 100 m, which in the literature is known to correspond to an area with high productivity [35]. In addition, habitat quality is higher in summer months than in winter months. This may be due to a winter decrease in upwelling and consequently to the decrease of the common dolphins' most important preys as the sardines [36]. Therefore, the seasonality in the habitat suitability is mostly related to prey biomass and water productivity.

Among the environmental predictors used in the model, the chlorophyll concentration has an important ecological role. It actually acts as a proxy for other biological elements: it is in fact known to reflect a high presence of pelagic schooling fish, such as the sardine (*Sardina pilchardus*), which is the most abundant pelagic schooling fish in the Portuguese coast. The distribution of this fish has been suggested to be correlated with chlorophyll concentration in our study area [37]. The contributions of each variable to the model were approximately: bathymetry 45 %, SST 31 %, slope 13 % and Chl-a 10 %. The contributions are quite balanced, and the bathymetry predictor has the biggest contribution, together with the temperature (SST).

Habitat suitability models gave an Area Under the Curve (AUC) of 0.88. AUC is a common normalized indicator that summarizes the information of the ROC (Receiver Operating Characteristic) curve and is widely used as a statistic index to assess the discriminatory ability of a species distribution model, giving a measure of its performance [38]. In practice, the AUC is the probability that a randomly chosen presence site will be ranked above a randomly chosen absence site. A random ranking has on average an AUC of 0.5, a score higher than 0.5 indicates better predictive accuracy of the model and a perfect ranking achieves the best possible AUC of 1.0. Models with values above 0.75 are considered potentially useful [33]. In general, maximum entropy models show very high-performance scores in the literature when predicting the niche of marine organisms compared to other ENMs and they were very often chosen in studies with the same purpose.

The comparison between Erbes' method and Bayes-based estimation method revealed similar risk distributions which is extremely relevant since it validates the Bayes-based method and consequently encourages its use in future risk assessment studies. Additionally, quantifying risk levels, through the Bayes method, makes it possible to compare risk results for different species in different places and times, since due to the probability normalization of the result it becomes an absolute comparable quantity, which was not possible with the method previously described by Erbe.

The results confirm the important impact that seismic surveys may have in species, suggesting that a way to diminish this impact is to take into account the effect of the seasons in the sound propagation and in species habitat quality, choosing those where the impact may be lower.

5 Conclusion

Seismic surveys inject important quantities of energy into the ocean and consequently put at risk marine species in the surrounding area. Seismic surveys are usually conducted to prospect oil and gas deposits but also to evaluate the viability of offshore structures installation, such as offshore wind farms.

In the framework of the JONAS project deliverable D8.3, this report intends to develop a tool to estimate the impact of noise resulting from a seismic survey in marine species. This tool was then used in the region of Setúbal, Portugal for the period of January and June 2019 to assess the impact of a seismic survey on the community of common dolphins.

A typical seismic survey scenario was designed near the Region of Setúbal and Habitat Suitability maps for the common dolphin were developed for both target months. This information was then used to estimate the potential risk that this species could be subjected to during a seismic survey.

The outcome of this report may be divided in three aspects: 1) underwater noise propagation, 2) species habitat suitability and 3) risk levels.

The results provided by this tool allow to draw some conclusions such as the fact that sound exposure levels in the area of the seismic survey may reach exceptionally high values impacting the temporary and permanent threshold shifts of hearing perception of various species in a range of about 40 km around the surveying zone.

The results led us to assume that there are periods of the year that are "more suitable" for seismic surveying than others and, for this reason, a previous evaluation of environmental factors of the target area as well as the HS for the species present in the area should always be taken into account.

To conclude, the proposed tool provides a first assessment of the shallow water seismic survey impact with quantifiable and comparable risk outputs, which may be used for area management decision support.

6 Acknowledgements

The authors would like to gratefully acknowledge the contribution of the WiMUST project (Widely scalable Mobile Underwater Sensor Technology) in the experimental evaluation of the seismic source characteristics used in this report.

Additionally, the authors gratefully acknowledge Whale-watching companies MarIlimitado from Sagres and SeaEo tours from Setubal for providing us with observation records for cetaceans. We are also very greatful to Hany Alonso and Joana Andrade from the Portuguese Society for the Study of Birds (SPEA) for giving us access to their dataset of cetaceans and seabirds along all the Portuguese coast. Finally, we are deeply grateful to Marc Fernández Morrón from the MARE-Madeira center, who gave a fundamental contribution in the Species Distribution Models creation as well as his support all along.

References

[1] F. Thomsen, S. Mendes, F. Bertucci, M. Breitzke, E. Ciappi, A. Cresci, E. Debusschere, C. Ducatel, T. Folegot, C. Juretzek, F.-P. Lam, J. O'Brien, and M. E. D. Santos, "Addressing Underwater Noise in Europe: Current State of Knowledge and Future Priorities," 2021.

[2] D. P. Nowacek, C. W. Clark, D. Mann, P. J. Miller, H. C. Rosenbaum, J. S. Golden, M. Jasny, J. Kraska, and B. L. Southall, "Marine seismic surveys and ocean noise: Time for coordinated and prudent planning," *Frontiers in Ecology and the Environment*, vol. 13, no. 7, pp. 378–386, 2015.

[3] N. Kukreja, M. Louboutin, M. Lange, F. Luporini, and G. Gorman, "Rapid Development of Seismic Imaging Applications Using Symbolic Math," in *Third EAGE Workshop on High Performance Computing for Upstream*, 2017.

[4] Offshore Magazzine, "Portugal signs concessions for offshore exploration," 2007.

[5] ENMC, "Pesquisa de Petróleo em Portugal," tech. rep., 2016.

[6] L. Castro-Santos, D. Silva, A. R. Bento, N. Salvação, and C. Guedes Soares, "Economic feasibility of floating offshore wind farms in Portugal," *Ocean Engineering*, vol. 207, no. April, 2020.

[7] D. Silva, P. Martinho, and C. G. Soares, "Wave energy Distribution along the Portuguese continental coast based on A thirty three years hindcast," *Renewable Energy*, vol. 127, 2018.

[8] A. M. Correia, P. Tepsich, M. Rosso, R. Caldeira, and I. Sousa-Pinto, "Cetacean occurrence and spatial distribution: Habitat modelling for offshore waters in the Portuguese EEZ (NE Atlantic)," *Journal of Marine Systems*, vol. 143, pp. 73–85, Mar. 2015.

[9] P. Weatherall, K. Marks, M. Jakobsson, T. Schmitt, S. Tani, J. Arndt, M. Rovere, D. Chayes, V. Ferrini, and R. Wigley, "A new digital bathymetric model of the world's oceans.," *Earth and Space Science*, vol. 2, pp. 331–345, 2015.

[10] C. Soares, F. Zabel, and S. M. Jesus, "A shipping noise prediction tool," in *MTS/IEEE OCEANS 2015 - Genova: Discovering Sustainable Ocean Energy for a New World*, (Genova, Italy), pp. 1–7, 2015.

[11] L. F. D. ARRUDA, P. E. MARTINS, A. F. da SILVA, J. E. R. de MORAES, P. VAZ-PIRES, R. O. de Almeida OZÓRIO, and M. OETTERER, "The fishery sector in portugal - report study," *Boletim do Instituto de Pesca*, vol. 37, no. 2, pp. 199–207, 2018.

[12] P. K. Trabant, "Seismic sources," *International Geophysics*, vol. 58, no. C, pp. 310–356, 1995.

[13] R. E. Sheriff, *Encyclopedic Dictionary of Exploration Geophysics*. Tulsa, 1991.

[14] Y. Pei, G. Kan, L. Zhang, Y. Huang, Z. Liu, B. Liu, and K. Yan, "Characteristics of source wavelets generated by two sparkers," *Journal of Applied Geophysics*, vol. 170, p. 103819, 2019.

[15] S. M. Jesus, "FOT - a tool for geoacoustic survey planning and resources optimization," tech. rep., Universidade do Algarve, Faro, 2018.

[16] M. B. Porter and E. L. Reiss, "A numerical method for ocean acoustic normal modes.," *Journal of the Acoustical Society of America*, vol. 76, no. 1, 1984.

[17] R. Duarte, G. Spadoni, C. Soares, and S. M. Jesus, "Anthropogenic noise prediction for light seismic surveys off the SW coast of Portugal," in *OCEANS 2021: San Diego – Porto, 2021*, pp. 1–6, 2021.

[18] S. J. Phillips, R. P. Anderson, and R. E. Schapire, "Maximum entropy modeling of species geographic distributions," *Ecological Modelling*, vol. 190, pp. 231–259, Jan. 2006.

[19] B. Naimi, "usdm: Uncertainty Analysis for Species Distribution Models. R Package Version 1.," 2015.

[20] X. Feng, D. S. Park, Y. Liang, R. Pandey, and M. Papeş, "Collinearity in ecological niche modeling: Confusions and challenges," *Ecology and Evolution*, vol. 9, no. 18, pp. 10365–10376, 2019. _eprint: https://onlinelibrary.wiley.com/doi/pdf/10.1002/ece3.5555.

[21] M. E. Aiello-Lammens, R. A. Boria, A. Radosavljevic, B. Vilela, and R. P. Anderson, "spThin: an R package for spatial thinning of species occurrence records for use in ecological niche models," vol. Ecography 38, 541–545., 2015.

[22] W. F. Ponder, G. A. Carter, P. Flemons, and R. R. Chapman, "Evaluation of Museum Collection Data for Use in Biodiversity Assessment," *Conservation Biology*, vol. 15, no. 3, pp. 648–657, 2001. _eprint: https://onlinelibrary.wiley.com/doi/pdf/10.1046/j.1523-1739.2001.015003648.x.

[23] M. Fernandez, C. Yesson, A. Gannier, P. I. Miller, and J. M. Azevedo, "The importance of temporal resolution for niche modelling in dynamic marine environments," *Journal of Biogeography*, vol. 44, no. 12, pp. 2816–2827, 2017. _eprint: https://onlinelibrary.wiley.com/doi/pdf/10.1111/jbi.13080.

[24] A. K. Darracq and J. Tandy, "Misuse of Habitat Terminology by Wildlife Educators, Scientists, and Organizations," *The Journal of Wildlife Management*, vol. 83, no. 4, pp. 782–789, 2019. _eprint: https://onlinelibrary.wiley.com/doi/pdf/10.1002/jwmg.21660.

[25] G. Wang, C. Wang, Z. Guo, L. Dai, Y. Wu, H. Liu, Y. Li, H. Chen, Y. Zhang, Y. Zhao, H. Cheng, T. Ma, and F. Xue, "Integrating Maxent model and landscape ecology theory for studying spatiotemporal dynamics of habitat: Suggestions for conservation of endangered Red-crowned crane," *Ecological Indicators*, vol. 116, p. 106472, Sept. 2020.

[26] C. Erbe, C. Reichmuth, K. Cunningham, K. Lucke, and R. Dooling, "Communication masking in marine mammals: A review and research strategy," *Marine Pollution Bulletin*, vol. 103, no. 1-2, pp. 15–38, 2016.

[27] N. D. Merchant, R. C. Faulkner, and R. Martinez, "Marine Noise Budgets in Practice," *Conservation Letters*, vol. 11, no. 3, pp. 1–8, 2018.

[28] E. Verling, R. Miralles Ricós, M. Bou-Cabo, G. Lara, M. Garagouni, J. M. Brignon, and T. O'Higgins, "Application of a risk-based approach to continuous underwater noise at local and subregional scales for the Marine Strategy Framework Directive," *Marine Policy*, vol. 134, no. September, p. 104786, 2021.

[29] A. Farcas, P. M. Thompson, and N. D. Merchant, "Underwater noise modelling for environmental impact assessment," *Environmental Impact Assessment Review*, vol. 57, pp. 114–122, 2016.

[30] C. Erbe, R. Williams, D. Sandilands, and E. Ashe, "Identifying modeled ship noise hotspots for marine mammals of Canada's Pacific region," *PLoS ONE*, vol. 9, no. 3, pp. 1–10, 2014.

[31] V. Popov and V. Klishin, "EEG study of hearing in the common dolphin, Delphinus delphis," *Aquatic Mammals*, vol. 24, no. 1, pp. 13–20, 1998.

[32] M. A. Silva, "Diet of common dolphins, Delphinus delphis, off the Portuguese continental coast," *Journal of the Marine Biological Association of the United Kingdom*, vol. 79, pp. 531–540, June 1999. Publisher: Cambridge University Press.

[33] S. J. Phillips and M. Dudík, "Modeling of species distributions with Maxent: new extensions and a comprehensive evaluation," *Ecography*, vol. 31, no. 2, pp. 161–175, 2008. _eprint: https://onlinelibrary.wiley.com/doi/pdf/10.1111/j.0906-7590.2008.5203.x.

[34] J. J. Finneran, "Auditory Weighting Functions and TTS/PTS Exposure Functions for Marine Mammals Exposed to Underwater Noise," tech. rep., Space and Naval Warfare Systems Center Pacific San Diego United States, 2016.

[35] P. P. W. Yen, W. J. Sydeman, and K. D. Hyrenbach, "Marine bird and cetacean associations with bathymetric habitats and shallow-water topographies: implications for trophic transfer and conservation," *Journal of Marine Systems*, vol. 50, pp. 79–99, Sept. 2004.

[36] T. A. Jefferson, D. Fertl, J. Bolaños-Jiménez, and A. N. Zerbini, "Distribution of common dolphins (Delphinus spp.) in the western Atlantic Ocean: a critical re-examination," *Marine Biology*, vol. 156, pp. 1109–1124, May 2009.

[37] A. E. Moura, N. Sillero, and A. Rodrigues, "Common dolphin (Delphinus delphis) habitat preferences using data from two platforms of opportunity," *Acta Oecologica*, vol. 38, pp. 24–32, Jan. 2012.

[38] A. Jiménez-Valverde, "Insights into the area under the receiver operating characteristic curve (AUC) as a discrimination measure in species distribution modelling," *Global Ecology and Biogeography*, vol. 21, no. 4, pp. 498–507, 2012. _eprint: https://onlinelibrary.wiley.com/doi/pdf/10.1111/j.1466-8238.2011.00683.x.

[39] S. B. Martin, C. Morris, K. Bröker, and C. O'Neill, "Sound exposure level as a metric for analyzing and managing underwater soundscapes," *The Journal of the Acoustical Society of America*, vol. 146, no. 1, pp. 135–149, 2019.

A Sound Exposure Level definition

Sound exposure level (SEL) is a measure of sound energy that takes into account both received sound pressure level (SPL), and the duration of the exposure. SEL is an important metric for quantifying sound effect on marine life. SEL is defined from the recording of SPL over time by: 1) taking the maximum of a given event; 2) determining the interval of time around the peak where the recording is within 10 dB from the maximum level and 3) integrating the signal energy in that interval. In equations this may be written as [39]:

$$SEL[dBre1\mu Pa^2 s] = 10log_{10}\frac{T}{T_0}\left[\frac{1}{T}\int_t^{t+T}\frac{p^2(\tau)}{p_0^2}d\tau\right], \tag{8}$$

where the integral in brackets is the SPL, T_0 and p_0 are the reference time interval and reference acoustic pressure, taken as 1s and $1\mu Pa$, respectively, and the interval $[t, t+T]$ is determined as the values of the SPL within 10 dB of the maximum in a given recording. Taking into account the reference values and previous definitions another, possible simpler, way to write (8) is:

$$SEL[dBre1\mu Pa^2 s] = 10log_{10}T + SPL \tag{9}$$

Sometimes it is useful to define the so-called single strike SEL (SEL_{ss}) for one pulse, that can be pile driving or air gun shot, and cumulative SEL (SEL_{cum}) as a sum of multiple strikes which, if the SEL of individual strikes are assumed approximately equal along time, the cumulative SEL may be given by:

$$SEL_{cum} = 10log_{10}(N \times 10^{SEL_{ss}/10}) = SEL_{ss} + 10log_{10}(N) \tag{10}$$

B Species in Portuguese waters

The following appendix section show three categories of species present in Portuguese waters: a) sea turtles, b) marine invertebrates and c)fishes according to the FAO [8]. The highlighted species are those who are interesting under an acoustic point of view. Among the highlighted ones, species in bold and darker yellow are those that had enough records (in the target area and for the selected time span considered in this study) to allow the creation of density maps.

Common name	***Scientific name***
Green turtle	*Chelonia mydas*
Hawksbill turtle	*Eretmochelys imbricata*
Kemp's ridley turtle	*Lepidochelys kempii*
Leatherback turtle	*Dermochelys coriacea*
Loggerhead turtle	***Caretta caretta***

Figure 19: Table of sea turtles in Portuguese waters.

[8] https://www.fao.org/

Common name	***Scientific name***	**Common name**	***Scientific name***
Bigeye cranch squid	*Liguriella podophthalma*	Lyre cranch squid	*Bathothauma lyromma*
Blue and red shrimp	*Aristeus antennatus*	Melancholy cranch squid	*Sandalops melancholicus*
Blue mussel	***Mytilus edulis***	Midsize squid	*Alloteuthis media*
Broadtail shortfin squid	*Illex coindetii*	Musky octopus	*Eledone moschata*
Caramote prawn	*Penaeus kerathurus*	Neon flying squid	*Ommastrephes bartramii*
Carol bobtail squid	*Neorossia caroli*	**Norway lobster**	***Nephrops norvegicus***
Common clubhook squid	*Onychoteuthis banksii*	Northern quahog (hard clam)	*Mercenaria mercenaria*
Common bobtail squid	*Sepietta oweniana*	Odd bobtail squid	*Heteroteuthis dispar*
Common shrimp	*Crangon crangon*	Pacific cupper oyster	*Crassostrea gigas*
Dana octopus squid	*Taningia danae*	Palmate octopus	*Tremoctopus violaceus*
Deep-water rose shrimp	*Parapenaeus longirostris*	Peacock cranch squid	*Taonius pavo*
Diamondback squid	*Thysanoteuthis rhombus*	Pink cuttlefish	*Sepia orbignyana*
Edible crab	*Cancer pagurus*	Ram's horn squid	*Spirula spirula*
Elegant cuttlefish	*Sepia elegans*	Reverse jewell squid	*Histioteuthis reversa*
Elegant bobtail squid	*Sepietta neglecta*	Roundear enope squid	*Pterygioteuthis giardi*
European common squid	*Alloteuthis subulata*	Ruppell's octopus squid	*Octopoteuthis sicula*
European flying squid	*Todarodes sagittatus*	Sharper enope squid	*Ancistrocheirus lesueurii*
European lobster	*Homarus gammarus*	Stauroteuthis syrtensis	*Stauroteuthis syrtensis*
European squid	*Loligo vulgaris*	Stout bobtail squid	*Rossia macrosoma*
Glassy flying squid	*Hyaloteuthis pelagica*	Striped venus	*Chamelea gallina*
Great atlantic scallop	*Pecten maximus*	Toothed-fin squid	*Chtenopteryx sicula*
Greater argonaut	*Argonauta argo*	Tuberculate octopus	*Ocythoe tuberculata*
Horned octopus	*Eledone cirrhosa*	Umbrella squid	*Histioteuthis bonnellii*
Jewel enope squid	*Pyroteuthis margaritifera*	Unarmed cranch squid	*Egea inermis*
Lentil bobtail squid	*Rondeletiola minor*	Unihorn octopus	*Scaeurgus unicirrhus*
Liocranchia reinhardti	*Liocranchia reinhardti*	Veined squid	*Loligo forbesii*
Long armed squid	*Chiroteuthis veranii*	Whale squid	*Walvisteuthis virilis*

Figure 20: Table of invertebrates in Portuguese waters.

Common name	*Scientific name*	Common name	*Scientific name*	Common name	*Scientific name*
Atlantic mackerel	*Scomber scombrus*	European sprat	*Sprattus sprattus*	Picked dogfish	*Squalus acanthias*
Atlantic horse mackerel	*Trachurus trachurus*	False catshark	*Pseudotriakis microdon*	Pink dentex	*Dentex gibbosus*
Atlantic wolffish	*Anarhichas lupus*	Electric ray	*Torpedo nobiliana*	Portuguese dogfish	*Centroscymnus coelolepis*
Atlantic sawtail catshark	*Galeus atlanticus*	Flathead gray mullet	*Mugil cephalus*	Porbeagle	*Lamna nasus*
Basking shark	*Cetorhinus maximus*	Frigate tuna	*Auxis thazard*	Pouting (=bib)	*Trisopterus luscus*
Bigeye thresher	*Alopias superciliosus*	Frilled shark	*Chlamydoselachus anguineus*	Rabbit fish	*Chimaera monstrosa*
Bigeye sixgill shark	*Hexanchus nakamurai*	Gilthead seabream	*Sparus aurata*	Red mullet	*Mullus barbatus*
Birdbeak dogfish	*Deania calcea*	Goblin shark	*Mitsukurina owstoni*	Redbanded seabream	*Pagrus auriga*
Black dogfish	*Centroscyllium fabricii*	Goldblotch grouper	*Epinephelus costae*	Roughtail stingray	*Dasyatis centroura*
Black cusk-eel	*Genypterus maculatus*	Great hammerhead	*Sphyrna mokarran*	Roundnose grenadier	*Coryphaenoides rupestris*
Black scabbardfish	*Aphanopus carbo*	Great lanternshark	*Etmopterus princeps*	Sandbar shark	*Carcharhinus plumbeus*
Blackchin guitarfish	*Rhinobatos cemiculus*	Great white shark	*Carcharodon carcharias*	Sailfin roughshark	*Oxynotus paradoxus*
Blonde ray	*Raja brachyura*	Hagfish	*Myxine glutinosa*	Scalloped hammerhead	*Sphyrna lewini*
Blacktailed spurdog	*Squalus melanurus*	**John dory**	***Zeus faber***	Shortfin mako	*Isurus oxyrinchus*
Blackmouth catshark	*Galeus melastomus*	Kitefin shark	*Dalatias licha*	Shortnose spurdog	*Squalus megalops*
Blue ling	*Molva dypterygia*	Knifetooth dogfish	*Scymnodon ringens*	Silky shark	*Carcharhinus falciformis*
Blue marlin	*Makaira nigricans*	Large-eyed rabbitfish	*Hydrolagus mirabilis*	Silver scabbadfish	*Lepidopus caudatus*
Blue shark	*Prionace glauca*	Largehead hairtail	*Trichiurus lepturus*	Skipjack tuna	*Katsuwonus pelamis*
Blue whiting	*Micromesistius poutassou*	Large-eye dentex	*Dentex macrophthalmus*	Small-eyed ray	*Raja microocellata*
Blue spotted seabream	*Pagrus caeruleostictus*	Lemon sole	*Microstomus kitt*	**Small spotted catshark**	***Scyliorhinus canicula***
Bobo croaker	*Pseudotolithus elongatus*	Leafscale gulper shark	*Centrophorus squamosus*	Smalleyed rabbitfish	*Hydrolagus affinis*
Bluntnose sixgill shark	*Hexanchus griseus*	Little sleeper shark	*Somniosus rostratus*	Smooth lanternshark	*Etmopterus pusillus*
Bramble shark	*Echinorhinus brucus*	Ling	*Molva molva*	Smooth hammerhead	*Sphyrna zygaena*
Brown ray	*Raja miraletus*	Little tunny	*Euthynnus alletteratus*	Smoothback angel shark	*Squatina oculata*
Bullet tuna	*Auxis rochei*	Longfin mako	*Isurus paucus*	Spotted ray	*Raja montagui*
Bull ray	*Pteromylaeus bovinus*	Longnose spurdog	*Squalus blainville*	Spiny butterfly ray	*Gymnura altavela*
Common dab	*Limanda limanda*	Longnose velvet dogfish	*Centroscymnus crepidater*	Starry smooth-hound	*Mustelus asterias*
Common dentex	*Dentex dentex*	Lowfin gulper shark	*Centrophorus lusitanicus*	Strainghtnose rabbit fish	*Rhinochimera atlantica*
Common stingray	*Dasyatis pastinaca*	Lumpfish (lumpsucker)	*Cyclopterus lumpus*	Swordfish	*Xiphias gladius*
Common sole	*Solea solea*	Lusitanian cownose ray	*Rhinoptera marginata*	Surmullet	*Mullus surmuletus*
Common torpedo	*Torpedo torpedo*	Lyconus brachycolus	*Lyconus brachycolus*	Sturgeon	*Acipenser sturio*
Common sawfish	*Pristis pristis*	Mediterrean horse mackerel	*Trachurus mediterraneus*	Thornback ray	*Raja clavata*
European anchovy	*Engraulis encrasicolus*	Marbled electric ray	*Torpedo marmorata*	Thresher	*Alopias vulpinus*
European conger	*Conger conger*	Megrim	*Lepidorhombus whiffiagonis*	Tope shark	*Galeorhinus galeus*
European flounder	*Platichthys flesus*	Morocco dentex	*Dentex maroccanus*	Undulate ray	*Raja undulata*
European hake	*Merluccius merluccius*	Mouse catshark	*Galeus murinus*	Velvet belly	*Etmopterus spinax*
European pilchard (sardine)	*Sardina pilchardus*	Nursehound	*Scyliorhinus stellaris*	Whale shark	*Rhincodon typus*
European plaice	*Pleuronectes platessa*	Oceanic whitetip shark	*Carcharhinus longimanus*	White seabream	*Diplodus sargus*
European seabass	***Dicentrarchus labrax***	Orange roughy	*Hoplostethus atlanticus*	Yellowfin tuna	*Thunnus albacares*

Figure 21: Table of fishes in Portuguese waters.